



HAL
open science

Potential combined impacts of climate change and non-indigenous species arrivals on Bay of Biscay trophic network structure and functioning

M. Le Marchand, F. Ben Rais Lasram, E. Araignous, B. Saint-Béat, Géraldine Lassalle, N. Michelet, S. Serre, G. Safi, M. Lejart, N. Niquil, et al.

► To cite this version:

M. Le Marchand, F. Ben Rais Lasram, E. Araignous, B. Saint-Béat, Géraldine Lassalle, et al.. Potential combined impacts of climate change and non-indigenous species arrivals on Bay of Biscay trophic network structure and functioning. *Journal of Marine Systems*, 2022, 228, pp.103704. 10.1016/j.jmarsys.2022.103704 . hal-03557393

HAL Id: hal-03557393

<https://hal.inrae.fr/hal-03557393>

Submitted on 22 Jul 2024

HAL is a multi-disciplinary open access archive for the deposit and dissemination of scientific research documents, whether they are published or not. The documents may come from teaching and research institutions in France or abroad, or from public or private research centers.

L'archive ouverte pluridisciplinaire **HAL**, est destinée au dépôt et à la diffusion de documents scientifiques de niveau recherche, publiés ou non, émanant des établissements d'enseignement et de recherche français ou étrangers, des laboratoires publics ou privés.



Distributed under a Creative Commons Attribution - NonCommercial 4.0 International License

1 **Potential combined impacts of climate change and non-indigenous**
2 **species arrivals on Bay of Biscay trophic network structure and**
3 **functioning**

4 Le Marchand M.^{1,2}, Ben Rais Lasram F.³, Araignous E.², Saint-Béat B.⁴, Lassalle G.⁵, Michelet
5 N.², Serre S.¹, Safi G.², Lejart M.², Niquil N.⁶ and Le Loc'h F.¹

6 ¹ *Univ Brest, CNRS, IRD, Ifremer, LEMAR, F-29280 Plouzané, France*

7 ² *France Energies Marines, 525 avenue Alexis de Rochon, 29280 Plouzané, France.*
8 *Marie.Lemarchand@univ-brest.fr*

9 ³ *Univ. Littoral Côte d'Opale, Univ. Lille, CNRS, UMR 8187, LOG, Laboratoire d'Océanologie et de*
10 *Géosciences, F 62930 Wimereux, France. frida.lasram@univ-littoral.fr*

11 ⁴ *IFREMER, Dyneco Pelagos, BP 70, 29208 Plouzané, France*

12 ⁵ *INRAE, UR EABX, 50 avenue de Verdun, Cestas Cedex 33612, France*

13 ⁶ *Lab BOREA, Team Ecofunc, Université de Caen, CNRS, MNHN, IRD, SU, UA CS 14032, 14000 Caen,*
14 *France. nathalie.niquil@unicaen.fr*

15

16 **Abstract**

17 The consequences of climate change for marine organisms are now well-known, and include
18 metabolism and behavior modification, distribution area shifts and changes in the
19 community. In the Bay of Biscay, the potential environmental niches of subtropical non-
20 indigenous species (NIS) are projected to expand as a response to sea temperature rise by
21 the mid-century under the RCP8.5 climate change scenario. In this context, this study aims to
22 project the combined effects of changes in indigenous species distribution and metabolism
23 and NIS arrivals on the functioning of the Bay of Biscay trophic network. To do this, we
24 created six different Ecopath food web models: a “current situation” trophic model (2007–
25 2016) and five “future” trophic models. The latter five models included various NIS biomass
26 combinations to reflect different potential scenarios of NIS arrivals. For each model, eight
27 Ecological Network Analysis (ENA) indices were calculated, describing the properties of the
28 food web resulting from the sum of interactions between organisms. Our results illustrate
29 that rising temperature increases the quantity of energy passing through the system due to
30 increased productivity. A decrease in the biomass of some trophic groups due to the
31 reduction of their potential environmental niches also leads to changes in the structure of
32 the trophic network. The arrival of NIS is projected to change the fate of organic matter
33 within the ecosystem, with higher cycling, relative ascendancy, and a chain-like food web. It
34 could also cause new trophic interactions that could lead to competition and thus modify
35 the food-web structure, with lower omnivory and higher detritivory. The combined impacts
36 (increasing temperatures and NIS arrivals) could lower the resilience and resistance of the
37 system.

38

39 **Key words:** climate change, non-indigenous species, Ecological Network Analysis, food web
40 modeling, fisheries
41

42 **1. Introduction**

43 The impacts of climate change on marine biodiversity and ecosystem functioning have
44 been extensively studied over the last two decades (Harvell et al., 2002; Poloczanska et al.,
45 2013; Lenoir et al., 2020). At the global scale, several studies have predicted the effects of
46 climate change on marine ecosystems (Parmesan and Yohe, 2003; Butchart et al., 2010;
47 Poloczanska et al., 2013; Lotze et al., 2019), but there remains a need for local studies that
48 take into account environmental drivers in order to adapt management policies (Lopez y
49 Royo et al., 2009; Riera et al., 2016), especially in coastal areas already subject to different
50 human-induced pressures (eutrophication, fishing, recreational activities, pollution, marine
51 structures such as windfarms, etc.). Furthermore, climate change is expected to have greater
52 impacts on coastal areas than on the open ocean (Wong et al., 2014). As a consequence of
53 rising temperatures and the arrival of subtropical species (Cheung et al., 2012), marine
54 communities in temperate coastal areas are increasingly subject to tropicalization (Vergés et
55 al., 2014; Montero-Serra et al., 2015).

56 The Bay of Biscay is located in the northeastern part of the Atlantic Ocean, along the
57 west coast of France, in temperate latitudes already affected by warming temperatures
58 (Michel et al., 2009; Irigoien et al., 2011; Costoya et al., 2015). This temperature change has
59 induced a modification in local fish communities, with decreasing abundance and a shift in
60 distribution range (Costoya et al., 2015; Iglésias and Lorange, 2016; Delgado et al., 2018).
61 Indeed, a recent study projecting the potential environmental niches of 163 indigenous
62 species revealed that some of these species would shift westward or northward by 2050
63 under scenarios RCP2.6 and RCP8.5 (Le Marchand et al., 2020). This study also projected the
64 arrival of southern non-indigenous species (NIS) in the Bay of Biscay as a consequence of a
65 northward shift of their native ranges. A major limitation of this study, however, was that it
66 did not consider trophic interactions. Indeed, trophic interactions among species create a
67 complex network of fluxes, as a result of organism feeding suitability, such as in terms of
68 predation or herbivory (Montoya et al., 2006). There is now evidence that warming
69 temperatures affect ecosystem trophic dynamics (Lercari et al., 2018; Kwiatkowski et al.,
70 2019; Baird et al., 2019), notably due to the effects of trophic cascades (Doney et al., 2012).
71 Furthermore, it has been proven that the arrival of invasive species may alter the structure
72 and functioning of food webs (Baxter et al., 2004; Nehls et al., 2006; Baird et al., 2012).
73 However, to our knowledge, there are very few studies on the consequences for a local
74 trophic network of the arrival of NIS due to a shift of their distribution area under climate
75 change, in a temperate ecosystem (Moullec et al., 2019a).

76
77 In the Bay of Biscay, Le Marchand et al. (2020) revealed that under the RCP8.5
78 scenario, 54% of fish and cephalopod species would not undergo any range shift by 2050. .
79 These authors defined NIS as species currently beyond the southern border of the Bay of
80 Biscay and whose area of presence is projected to expand with climate change. These are
81 not invasive species *sensu stricto* (i.e., introduced by humans, having no predators,

82 opportunistic, and capable of rapid and dramatic increases in abundance; Mack et al., 2000).
83 In the context of climate change, little work has been done on the combined impacts of
84 changes on (1) indigenous species distribution and metabolism, and (2) NIS arrivals affecting
85 trophic network properties. These aspects are, nevertheless, crucial for ecosystem
86 management and policies (Halpern et al., 2015).

87 Given the impacts of climate change on the structure and functioning of marine
88 ecosystems, it is necessary to have reliable indicators that make it possible to follow and
89 anticipate ecosystem changes. Several types of indicators, such as Ecological Network
90 Analysis (ENA) indices, describe ecosystem functioning. Ecological network analysis provides
91 a set of indicators based on the analysis of the quantified flux (carbon or energy) within a
92 trophic network (Ulanowicz, 1986; Niquil et al., 2012). The main goal of these indicators is to
93 characterize the functioning of a system (Niquil et al., 1999) and to emphasize the holistic
94 properties of the food web (Fath et al., 2007). They make it possible to assess how the
95 trophic network may be modified following different changes in the ecosystem (Baird et al.,
96 1991). For instance, ENA indices can be used to explore how a system will evolve following
97 environmental change (Paar et al., 2019) or anthropogenic pressure (Bueno-Pardo et al.,
98 2018). In recent years, ENA indices have been proposed as highly promising indicators for
99 assessing the "Good Environmental Status" of marine ecosystems (Niquil et al., 2012),
100 targeted by the "Food Webs" descriptor of the Marine Strategy Framework Directive (Safi et
101 al., 2019; Fath et al., 2019) and proposed as tools for environmental managers (Schukel et
102 al., 2018).

103 The aim of the present study was to investigate the possible consequences of climate
104 change by coupling effects on indigenous species, consisting in a potential decrease in their
105 environmental niches and modifications to their metabolism, with the arrival of NIS in the
106 same area. The trophic functioning of the Bay of Biscay ecosystem was assessed by applying
107 various biological hypotheses for the mid-century and the RCP8.5 climate change scenario.
108 To do this, Ecopath models and ENA indicators were applied to the Bay of Biscay. To
109 consider the potential future NIS biomass, six models were built that progressively varied
110 the NIS biomass.

111

112 **2. Material and methods**

113 **2.1. Study area**

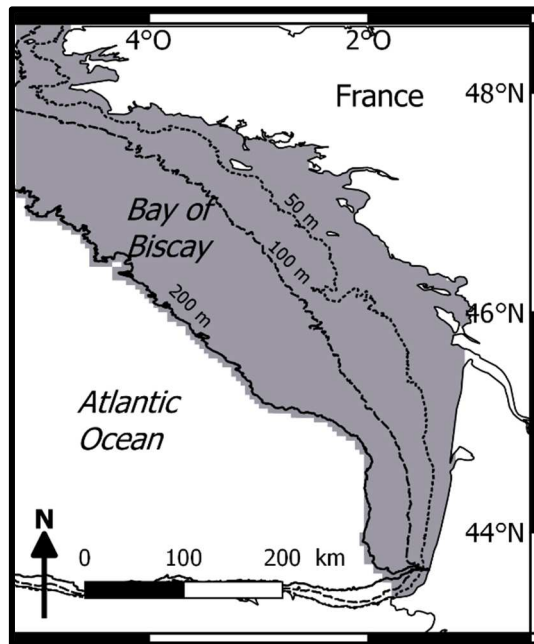


Figure 1: Geographical location of the study area: in grey, the French part of the Bay of Biscay continental shelf (30–200 meters depth)

The Bay of Biscay is a large gulf located on the Eastern side of the North Atlantic Ocean (Figure 1). It is bordered by the Spanish (43.5°N) and French coasts and by the English Channel and the Celtic Sea to the north (48.3°N). It is the top fishing area in Europe (ICES, 2020), with about 100,000 tonnes of fish and shellfish caught every year by French and other European fishermen (<http://ices.dk/marine-data>). Our study focused on the French part of the Bay of Biscay continental shelf (30–200 m depth). The Bay of Biscay is already affected by climate change, with its sea temperature in the upper 200 m layer increasing by $0.2^{\circ}\text{C}\cdot\text{decade}^{-1}$ between 1965 and 2004 (Michel et al., 2009) and general trends of changes in temperature seasonality have already been observed (Costoya et al., 2015). In addition, Chust et al. (2021) reported an increase in chlorophyll concentrations measured by satellite of $0.054\pm 0.012 \text{ mg m}^{-3} \text{ dec}^{-1}$ in the Bay of Biscay during the last two decades.

2.2. Ecopath model

The Ecopath with Ecosim (EwE) model is a tool used worldwide for modeling marine trophic networks. In this study, the 6.6 version of Ecopath was used. The Ecopath routine provides a snapshot of energy fluxes between different functional groups, from plankton to marine mammals (Christensen and Walters, 2004). A functional group is composed of one to several species with identical trophic behavior.

With Ecopath, the energy fluxes are modeled using two main equations. The first equation calculates production. It corresponds to the sum of all the outgoing fluxes and is defined as:

$$\text{Production} = \text{fishery catch} + \text{predation mortality} + \text{net migration} + \text{biomass accumulation} + \text{other mortalities}$$

142

143 Formally, for a functional group i and a predator j (j being a predator of i), this equation can
144 be written as:

145

$$146 \quad B_i \times (P/B)_i = Y_i + \sum_j (B_j \times (Q/B)_j \times DC_{ij}) + Ex_i + Bacc_i + B_i(1 - EE_i) \times (P/B)_i \quad (1)$$

147

148 where B is the biomass density ($t.km^{-2}$), P/B is the production rate ($year^{-1}$), Y is the
149 total catch ($t.km^{-2}$), Q/B is the consumption rate ($year^{-1}$), DC is the diet composition (DC_{ij} is
150 the proportion of i in the diet of j), Ex is the net migration rate ($year^{-1}$), $Bacc$ is the biomass
151 accumulation ($year^{-1}$), and EE is the ecotrophic efficiency (meaning the proportion of the
152 trophic group's biomass consumed by a predator or caught by fisheries).

153

154 The second equation represents the mass balance of the compartment, i.e., the inflows are
155 equal to the sum of the outflows of the compartment:

156

$$157 \quad \text{Consumption} = \text{production} + \text{respiration} + \text{unassimilated food}$$

158

159 Formally, this equation for a functional group i and a predator j (j being a predator of i) can
160 be written as:

161

$$162 \quad B_i \times (Q/B)_i = B_i \times (P/B)_i + R_i + U_i \quad (2)$$

163

164 where R is the respiration ($t.km^{-2}$) and U is the unassimilated food rate.

165

166 The models are then balanced by adjusting the EE when it is greater than 1. Indeed, the EE
167 represents the part of the group production that is consumed or fished, so it cannot be
168 higher than 1. The EE of each functional group was adjusted by modifying the predation
169 control in the diet composition matrix.

170

171 *2.3. The "Current" model, based on data from 2007–2016*

172 *2.3.1. Structure*

173 The "Current" model developed in this paper is composed of 52 compartments
174 ranging from detritus to mammals and seabirds. Among these, 44 compartments,
175 corresponding to species indigenous to the Bay of Biscay, were taken from a previous
176 Ecopath model (Moullec et al., 2017), itself based on a model by Lassalle et al. (2011). These
177 two models differ by their currency: wet weight for the former and carbon for the latter. We
178 used data from both models. Indeed, Moullec et al. (2017) used the values from Lassalle et
179 al. (2011), but chose to give their biomass in wet weight $t.km^2$, as did we. We primarily used
180 the data from Lassalle et al. (2011), except for those in $kgC.km$, for which we used the values
181 from Moullec et al. (2017), who converted those from Lassalle et al. In addition, we
182 performed some corrections in the composition of fish trophic groups and fisheries. Marine

183 mammals are divided into two groups according to their size. Seabirds are also divided into
184 two groups, according to their feeding strategies. There are 21 groups of fishes: two groups
185 of chondrichthyans (large piscivorous sharks and small sharks and rays), 11 monospecific
186 groups of fishes targeted by fisheries (seabass, blue whiting, hake, whiting, megrim, sole,
187 plaice, horse mackerel, sardine, anchovy, and pout) and eight multispecific groups:
188 anglerfishes (two species), mackerels (two species), flatfishes (benthos feeders), demersal
189 benthos feeders, demersal piscivores, demersal planktivores, pelagic piscivores, and pelagic
190 planktivores. Cephalopods are separated into two groups: benthic and pelagic. There are
191 eight benthic invertebrate groups (Norway lobster, lobsters/crabs, shrimps, carnivorous and
192 necrophagous benthic invertebrates, subsurface deposit feeding invertebrates, surface
193 suspension and deposit feeders, benthic meiofauna, and suprabenthic invertebrates).
194 Zooplankton are divided into three groups according to their size: microzooplankton (<200
195 μm), mesozooplankton (200–2000 μm), and macrozooplankton (>2000 μm). Phytoplankton
196 are divided into two groups (small and large), in addition to a primary benthic producers
197 group. There are also groups for bacteria, detritus, and discards.

198

199 In addition to these 44 compartments, we considered 8 groups of NIS fishes, which
200 were not included in the two previous models (Lassalle et al., 2011; Moullec et al., 2017).
201 They are composed of three monospecific groups of fishes targeted by fisheries in their
202 original habitat and that would potentially be targeted by the Bay of Biscay fisheries (hake,
203 *Merluccius senegalensis*; horse mackerel, *Trachurus trecae*; and gilt sardine, *Sardinella*
204 *aurita*) and five multispecific groups (flatfishes, demersal benthos feeders, demersal
205 piscivores, pelagic piscivores, and pelagic planktivores). Potential environmental niche
206 models run by Le Marchand et al. (2020) predicted the arrival of 57 NIS in the study area by
207 2050 under the IPCC RCP8.5 scenario. The NIS modeled in the present study are the same as
208 those modeled by Le Marchand et al. (2020) (Table S1 in the Supplementary data). These
209 species were selected because their current distribution areas are limited to northwest
210 Africa and are thus most likely to arrive in the Bay of Biscay.

211 NIS groups have the same preys and predators as those already present in the Bay of
212 Biscay, which we have named “mirror groups” in this study. Their diet proportions are
213 identical to their mirror groups.

214 The consistency of the Current model was checked with the Ecopath PREBAL tool (Link,
215 2010) (Figure S2 in the Supplementary data).

216

217 *2.3.2. Inputs in the Current model*

218 The current biomass of monospecific fish groups targeted by fisheries were calculated from
219 total biomass values given by Ifremer and reported in t.km^2 (Ifremer 2021), and averaged
220 over the 2007-2016 period. Due to a lack of data, the current biomass of the six multispecific
221 fish groups were estimated by Ecopath using an EE of 0.8 for the pelagic piscivorous group
222 and of 0.95 for the other groups (Table S3 in the Supplementary data). The current biomass
223 of large piscivorous sharks and small sharks and rays were estimated by Ecopath with EE

224 values of 0.6 and 0.8, respectively (Moullec et al., 2017). The diet matrix was obtained from
225 previous Ecopath models of the Bay of Biscay (Lassalle et al., 2011; Moullec et al., 2017).

226

227 To maintain the same structure for the different models, because ENA indices are
228 sensitive to model topology (Fath et al., 2013), the NIS were considered in the Current model
229 with a biomass close to 0 (i.e., 0.0001t.km⁻², Table 1). The diets of the NIS multispecific group
230 were the same as for their current mirror groups, due to a lack of information on the diets of
231 those species. The diets of the three monospecific NIS groups were compiled from Fishbase
232 (Froese and Pauly, 2021). The NIS group contribution to the diet of their predators was kept
233 very low.

234

235 The P/B and Q/B parameters were updated for all fish groups. The P/B ratios for a fish
236 species *i* were calculated with the empirical equation (Allen, 1971; Pauly, 1980) (Table S3 in
237 Supplementary data):

238

$$239 \quad P/B = M_i + F_i = (K_i^{0.65} \times L_{\infty_i}^{-0.279} \times T^{0.463}) + (Y_i / B_i) \quad (3)$$

240

241 where *K* is the growth parameter from the Von Bertalanffy growth function (year⁻¹) for each
242 species (Froese and Pauly, 2021), *L*_∞ is the asymptotic length (cm), *T* is the mean
243 temperature (°C) over the Current model period (i.e., 2007–2016), *Y* is the yield (kg.year⁻¹)
244 and *B* is the biomass (kg.year⁻¹). The temperature assigned depends on the species' vertical
245 habitat, which was provided by Le Marchand et al. (2020): 9.74°C for benthic and demersal
246 (bottom temperature), 11.66°C for benthopelagic (mean water column temperature), and
247 12.26°C for pelagic species (surface temperature).

248

249 For all fish groups, the Q/B ratios were calculated for a species *i*, with the empirical equation
250 (Palomares and Pauly, 1998) (Table S3 in the Supplementary data):

251

$$252 \quad \text{Log}_{10}(Q/B) = 6.37 - 1.5045 \times \text{log}_{10}T' - 0.168 \times \text{log}_{10}W_{\infty_i} + 0.1399 \times \text{Pf} + 0.2765 \times \text{HD} \quad (4)$$

253

254 where *T'* is the mean temperature of seawater calculated by 1000/(*T* + 273.75), *W*_∞ is the
255 asymptotic weight (g), and *Pf* and *HD* are two dimensionless variables (*Pf* = 0 for herbivorous
256 and detritivorous species, 1 for others; *HD* = 0 for carnivorous species, 1 for others).

257

258 As ENA indices are sensitive to model topology (Fath et al., 2013), the topology of all models
259 was standardized. So, the eight NIS groups were considered in the Current model. However,
260 their biomass was close to 0 (i.e., 0.0001t.km⁻², Table 1). The diets of the three monospecific
261 NIS groups were compiled from Fishbase (Froese and Pauly, 2021). Their proportion in their
262 predator's diet was kept low in the Current model, given the low biomass (due to absence)
263 of the group. The P/B and Q/B ratios of the NIS monospecific groups were calculated using
264 equations (3) and (4). For the five NIS multispecific groups (i.e., NIS flatfishes, NIS demersal
265 benthos feeders, NIS piscivores, demersal planktivores, and NIS pelagic planktivores), some

266 of the species in the groups had not been sufficiently documented to calculate the Q/B. So,
267 the choice was made to use the default P/Q ratio of 0.25 instead (Table S3 in the
268 Supplementary data) (Christensen et al., 2005).

269
270 Depending on the pertinence of the data they relied upon, the biomass for other EwE
271 functional groups were taken from Lassalle et al. (2011) and Moullec et al. (2015). The
272 detailed information is provided in Table 3 in the Supplementary data.

273
274 *2.3.3. Fisheries*

275 Landings data were obtained from the International Council for the Exploration of the
276 Sea (ICES; <http://ices.dk/marine-data/Pages/default.aspx>) for the period 2007 to 2016. To
277 obtain a more realistic Ecopath model, we integrated the 10 main French fleets operating in
278 the area: bottom trawlers targeting demersal fishes, purse seiners, bottom trawlers
279 targeting Norway lobster, gillnetters larger than 15 meters, pelagic trawlers targeting small
280 pelagic fishes, gillnetters smaller than 15 meters, pelagic trawlers targeting demersal fish,
281 long-liners and line vessels, pelagic trawlers targeting tuna, and Danish seine. Other
282 European fleets were also included, mostly from Spain (29% of catches from foreign ships),
283 the United Kingdom (10%), and Belgium (6%). This information was included in the ICES
284 data.

285 The proportions contributing to the landings by each fleet were calculated from
286 OBSMER reports (Fauconnet et al, 2011; Dubé et al, 2012; Cornou et al, 2013; 2015a; 2015b;
287 2016; 2017; 2018). ICES data provided the total biomass caught for each species per year.
288 We applied the percentage calculated from OBSMER to the ICES data and obtained for the
289 total biomass of each Ecopath group caught by every fleet from 2010 to 2016. The landings
290 inputs were annual means of these results.

291
292 Discards were calculated similarly to landings. Indeed, OBSMER reports include the
293 discard rates for each species and each fleet, from 2010 to 2016. These rates were applied to
294 the ICES catches to obtain annual mean discards over this period.

295
296 *2.4. Projections*

297 To study the effects of NIS arrivals, we developed a comparative approach by creating five
298 other Ecopath models based on different community changes caused by the arrival of NIS,
299 compared with the current situation (2007–2016). We built these models for the mid-
300 century period (2041–2050) under the IPCC scenario RCP8.5. While the previous version of
301 the work conducted by Le Marchand et al. (2020) was based on both RCP2.6 and RCP8.5, we
302 chose to focus only on the latter. Including RCP2.6 would have considerably increased the
303 number of models. Additionally, the aim of our study was to explore the effects of NIS arrival
304 on native communities, which would be limited under scenario RCP2.6 according to the
305 results from Le Marchand et al. (2020). Thus, we therefore chose to only work with RCP8.5.
306 Into these models, we integrated the impacts of climate change on Bay of Biscay species by

307 considering (i) the evolution of fish and cephalopod biomass (based on Chaalali et al., 2016)
308 due to the projected evolution (gain or loss) of their suitable habitat (calculated in Le
309 Marchand et al., 2020); and (ii) the changes in the organisms' production and consumption.
310 The five hypotheses of the future evolution of the Bay of Biscay food web illustrate both
311 climate change effects and variation in NIS biomass.

312

313 *2.4.1. The common basis of the five future models*

314 The five hypotheses simulate progressive variation of the NIS biomass, which is the
315 only parameter to change between the five models. The common basis of the five
316 hypotheses integrates the effects of climate change on fish and cephalopod distributions
317 predicted for the mid-century under RCP8.5 as presented in the previous section.

318

319 *Future biomass:* Species that are projected to show no range shift maintain the same
320 biomass as in the Current model. For the species that are projected to undergo a range loss
321 (Le Marchand et al., 2020), a proportional reduction in biomass is applied according to the
322 reduction in their potential environmental niche (called "ecological niche" in Le Marchand et
323 al., 2020) by 2050 under RCP8.5 (see Chaalali et al., 2016): anglerfishes (-3.12%), whiting (-
324 17.15%), megrim (-3.75%), plaice (-9.73%), flatfishes (-4.89%), demersal benthos feeders (-
325 0.21%), demersal piscivores (-18.64%), pelagic planktivores (-1.21%), and sharks and rays (-
326 0.07%) (Table S4 in the Supplementary data).

327 The biomass values of cephalopods, benthic invertebrates, zooplankton,
328 phytoplankton, and bacteria estimated by the Current model were used as inputs for the five
329 future hypotheses without any changes, since changes in their potential environmental
330 niches were not considered in this study.

331

332 *Future P/B and Q/B:* The future P/B and Q/B ratios of fishes were calculated using equations
333 (3) and (4) and considering the water temperature projected by mid-century under RCP8.5.
334 The latter has already been calculated by Le Marchand et al. (2020), based on information
335 taken from three general circulation models (GFDL, IPSL, and MPI) (Taylor et al., 2012). The
336 temperature depth was integrated to produce values for the different fish habitat depths:
337 10.03°C for benthic and demersal, 12.34°C for benthopelagic, and 13.03°C for pelagic
338 species. For groups with several species, the P/B and Q/B were averaged and weighted
339 according to the biomass of each species. The resulting P/B and Q/B differed from those of
340 the Current model (Table S5 in the Supplementary data), which integrates the effects of
341 climate change on metabolism.

342 For cephalopods, benthic invertebrates, zooplankton, and primary producers, we
343 decided to apply the same alterations (+2%) of P/B and Q/B ratios as those observed for
344 fishes. Thus, the differences between current and projected fish P/B and Q/B values were
345 calculated and it appeared that future P/B and Q/B were 2% greater than current values. As
346 a consequence, a 2% increase of the P/B and Q/B was applied to the cephalopods, benthic
347 invertebrates, zooplankton, and primary producers.

348 Finally, as mammals and seabirds are homeotherms, their P/B and Q/B ratios
349 remained unchanged in the climate change models.

350

351 *Fisheries:* For the future models, we hypothesized that fishing effort would be the same as in
352 the Current model. The NIS were hypothesized to be fished at the same rate and by the
353 same fleet as their mirror group. However, to take into account the European “zero discard”
354 objective, discards were set to zero in the 2050 models for species under quota.
355 Consequently, landed discards were added to the landings inputs.

356

357 *2.4.2. Specificities of the projection models*

358 The five hypotheses of the future evolution of the Bay of Biscay food web illustrate
359 both climate change effects and variation in NIS biomass.

360

361 *Model 1 – ClimOnly:* No NIS arrive in the Bay of Biscay. This model integrates only the effects
362 of climate change on the species present in the Current model in the Bay of Biscay (i.e.,
363 decrease in the biomass of certain fish species due to the reduction of their potential
364 environmental niches and increased P/B and Q/B ratios). For the ClimOnly model, the NIS
365 biomass were set at 0.0001 t.km⁻² and maintained at fully consumed (EE > 0.95) (Figure 2)
366 (Table S6 in the Supplementary data).

367

368 The following four models are based on the conditions of ClimOnly, to which we
369 added NIS parameters.

370

371 *Model 2 – NISPel:* Only pelagic NIS arrive in the Bay of Biscay, as they are expected to shift
372 more rapidly than demersal species in the Bay of Biscay under climate change. For the NISPel
373 model, the biomass of flatfishes and demersal NIS was set at 0.0001 t.km⁻² and the NIS
374 pelagic biomass was estimated by Ecopath, using an EE of 0.8 for piscivores and 0.95 for
375 other groups (Figure 2) (Table S7 in the Supplementary data).

376

377 *Model 3 – NISEqual:* In this model, we considered that the environmental niches freed by
378 indigenous species are immediately occupied by NIS with same trophic function. The NIS
379 arrivals counterbalance the loss of biomass due to species impacted by climate change in the
380 Bay of Biscay. The biomass values of the main functional groups remain the same as in the
381 ClimOnly model. As the groups impacted by climate change are mainly demersal and benthic
382 species, this hypothesis mostly models the arrival of demersal and benthic NIS. For the
383 NISEqual model, the NIS group biomass values were equal to the biomass reduction of their
384 mirror current trophic groups due to climate change (Figure 2) (Table S8 in the
385 Supplementary data).

386

387 *Model 4 – NISMax:* In this model, there is no restriction on NIS arrivals. The biomass values
388 are not a priori estimated but calculated by Ecopath by balancing the two model equations

389 ((1) and (2)). An EE of 0.8 is applied for pelagic piscivorous NIS and 0.95 for other groups, as
390 we supposed their EE would be the same as those of the indigenous groups (Table S9 in the
391 Supplementary data).

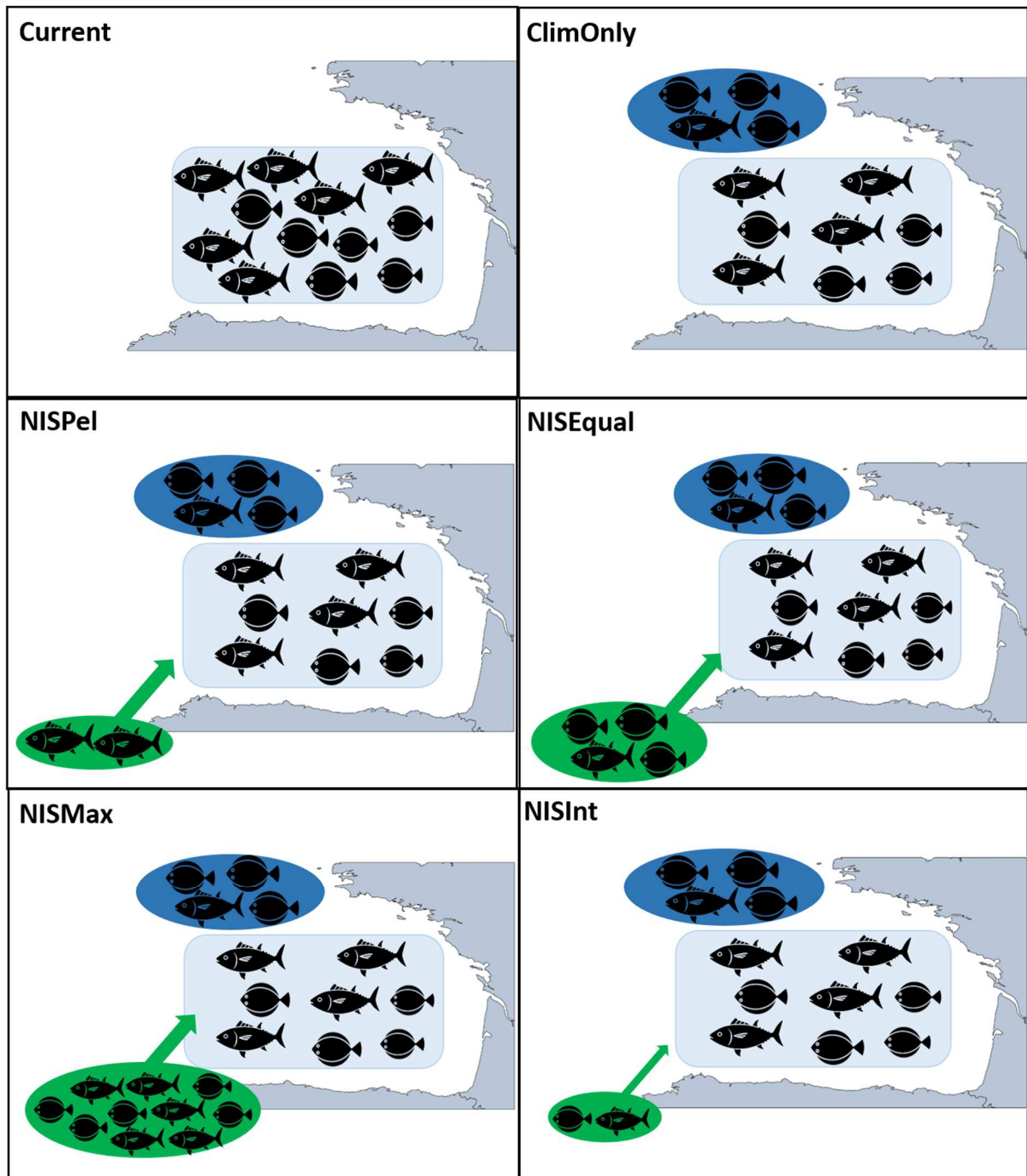
392

393 *Model 5 – NISInt*: This is a conservative option. A preliminary analysis of the potential
394 impacts of NISMax on the NIS biomass level estimate suggested that a good intermediate
395 situation between NISMax and other models would be obtained by dividing the NISMax
396 biomass by five (Figure 2).

397

398

399



400
401
402
403
404
405
406
407

Figure 2: Diagram showing the Current model (2007–2016) and the five projected models (2041–2050). The blue shapes represent the Bay of Biscay species (light blue for species not impacted by climate change and dark blue for species with a reduced biomass due to climate change). The green shapes represent non-indigenous species (NIS). The tuna-shaped symbol represent pelagic and benthopelagic species, the flatfish profile represents benthic and demersal species. The size of the green circle is relative to the NIS biomass.

2.5. ENA

408
409
410
411

Ecological network analysis (ENA) indices, which reveal the hidden properties of food webs, were used to highlight the effect of climate change and arrivals of new species in the Bay of Biscay. A set of five indices currently calculated in the Matlab routine ENATool

412 (Guesnet et al., 2015) were selected: Mean Trophic Level 2 (MTL₂), Total System Throughput
 413 (TST), Finn Cycling Index (FCI), relative ascendancy (A/C), and System Omnivory Index (SOI).
 414 In addition, three new indices (Averaged Mutual Information, AMI; Mean Trophic Level 3.25,
 415 MTL_{3.25}; and Detritivory/Herbivory ratio, D/H) added to this routine were calculated to
 416 provide a detailed description of food web structure and functioning (Table 2).

417 The Matlab routine ENATool takes into account Ecopath input uncertainties. It runs
 418 Monte-Carlo simulations to create a set of different versions of one Ecopath model, whose
 419 input parameters vary according to the Ecopath pedigree. The pedigree represents the
 420 coefficient of variation of every input and varies from 1 (the data are reliable) to 0 (the data
 421 estimated by Ecopath are not coherent) (Guesnet et al., 2015) (Table S11 in the
 422 Supplementary data). For each model, the ENATool routine created 100 simulations, varying
 423 the inputs for biomass and P/B and Q/B ratios, and the diet composition according to the
 424 pedigree. All simulations were balanced. For each model, we obtained 100 values for each
 425 ENA indicator.

426 The significant difference between the ENA values of each model was tested by a
 427 Kruskal–Wallis non-parametric test, as conditions of normality were not met. Then, the
 428 hypotheses were compared with each other using Dunn tests.

429 For greater clarity in the results, we separated the ENA indices into two groups according
 430 to what they reflected: network ENA (TST, FCI, AC, and AMI) and diet ENA (MTL₂, MTL_{3.25},
 431 SOI, and D/H).

432
 433 Table 1: Description of the ENA indices. T_{ij} is the flux from group i to group j ; TSTc is the sum of cycling fluxes;
 434 TL_i is the trophic level of group i ; B_i is the biomass of group i ; Q_i is the consumption of group i ; O_i is the omnivory
 435 index of group i ; D is the fluxes from detritus; Z_i is the import into the system through compartment i ; y_i is the
 436 output of the system from compartment i ; $T_{.j}$ is the flow to compartment j , DC_{ij} is the proportion of i in the diet
 437 of group j , and H is the flux from primary producers. The * specifies the indicators that were added to the basic
 438 ENATool routine.

Indicators	Definition	Formula	Interpretation of an increase in value
Total System Throughput (TST) /t.year ⁻¹ Ulanowicz (1986)	Sum of all fluxes in the system	$\sum_{ij} T_{ij} + z_i + y_i$	The overall activity of the system is increasing
Finn's Cycling Index (FCI) % Finn (1980)	Fraction of all system fluxes that are recycled	$\sum_j \frac{\sum_i T_{ij} + z_i}{TST}$	The system has more complex internal links, a better use of energy flowing through the system
Relative ascendancy (A/C), no units Ulanowicz (1986)	Quantification of the degree of organization of the system	$\frac{\sum_{i,j} T_{ij} \log\left(\frac{T_{ij} TST}{T_i t_j}\right)}{\sum_{i,j} T_{ij} \log\left(\frac{T_{ij}}{TST}\right)}$	The system has a higher degree of organization, the direct pathways are favored, chain-like
Averaged Mutual Information* (AMI), no units (Hirata and Ulanowicz,	Quantification of the exchange between compartments	$K \sum_{i,j} \left(\frac{T_{ij}}{TST}\right) T_{ij} \log\left(\frac{T_{ij} TST}{T_i t_j}\right)$	The system is more constrained and energy flows through particular pathways

1984)			
Mean Trophic Level 2 (MTL ₂), no units (Pauly, 1998)	Mean trophic level of consumers (all species with TL > 2)	$\frac{\sum_i TL_i \times B_i}{\sum_i B_i}$	The proportion of high trophic levels increases in the whole system
Mean Trophic Level 3.25* (MTL _{3.25}), no units Shannon et al. (2014)	Mean trophic level of predators (all species with TL > 3.25)	$\frac{\sum_i TL_i \times B_i}{\sum_i B_i}$	The proportion of the higher trophic levels has grown in the predators
System Omnivory Index (SOI), no units (Christensen et al., 1993)	Mean consumer omnivory index	$\frac{\sum_i \sum_j [TL_j \times (\sum_j TL_j \times DC_{ji})] \times \log T_{.j}}{\sum_i \log T_{.j}}$	The predators are less specialized. They feed on various trophic levels, this leads to more parallel flows in the system
Detritivory/Herbivory* (D/H) no units (Kay et al., 1989)	Ratio between detritivory and herbivory	$\sum Detritivory / \sum Herbivory$	A greater proportion of the system is supported by detritus

439

440

441 Moreover, we explored ENA index behavior according to the different models using a
 442 Principal Component Analysis (PCA). The PCA was performed with the *ade4* package for R
 443 Core Team 2019 software (v 3.6.1), with the ENA indices as variables and the models as
 444 individuals.

445

446 3. Results

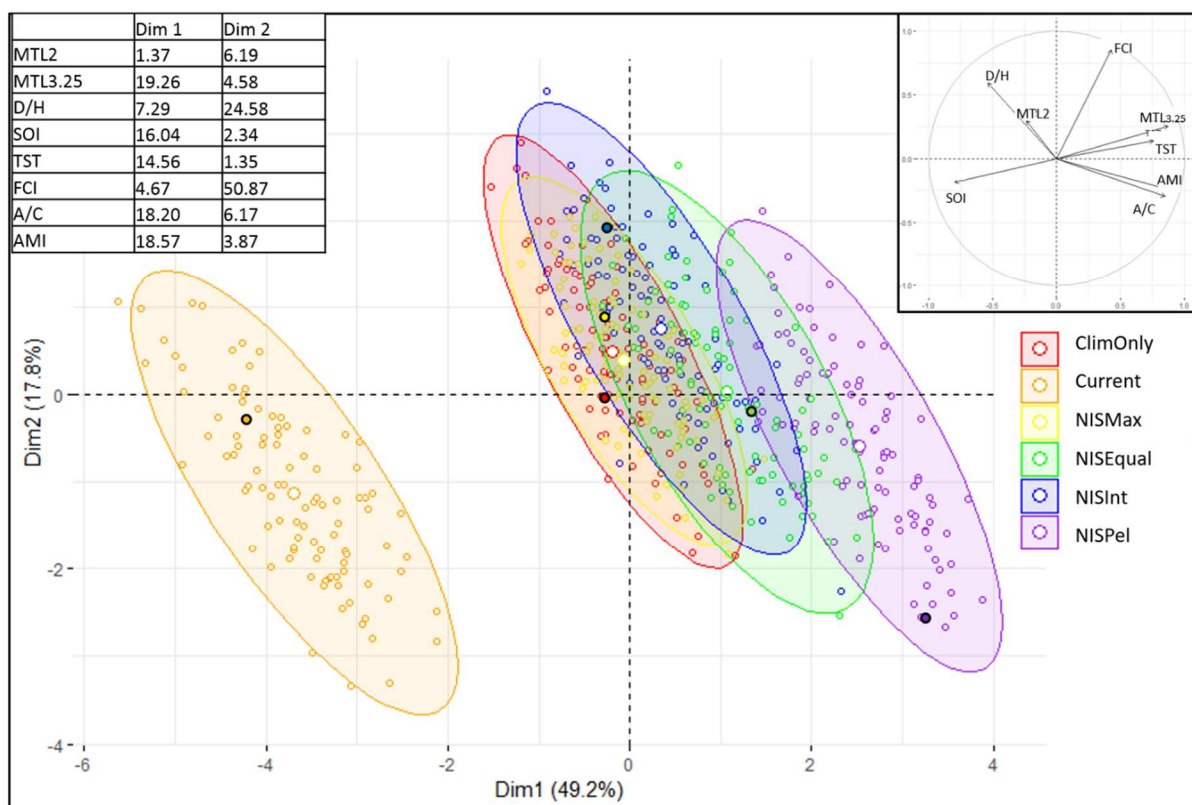
447 3.1. General trends

448 In the Current model, the trophic levels ranged from 1 to 4.49 (large pelagic sharks).
 449 Trophic Level (TL) I was composed of five groups (three groups of primary producers,
 450 detritus, and discards) and represented 63.59% of the total biomass. TL II encompassed
 451 heterotrophic bacteria, zooplankton, and some of the zoobenthos species, mainly
 452 subsurface deposit feeders; it represented 26.76% of the total biomass. TL III was composed
 453 of the majority of the fish groups (e.g., demersal piscivores *Trachurus trachurus*, *Solea solea*,
 454 etc.) and represented 9.29% of the total biomass. TL IV corresponded to top predators and
 455 represented only 0.96% of the total biomass.

456 3.2. ENA indices

457 The first two axes of the PCA (Figure 3) explain 69% of the variance, and only these are
 458 presented. The table on the top left of the figure gives information on the percentage
 459 contribution of each variable for each of the two dimensions. The first axis (horizontal:
 460 49.2% of the variance) is accounted for by the indices MTL_{3.25} (19.26%), AMI (18.57%), A/C
 461 (18.20%), SOI (16.04%), and TST (14.56%). The second axis (vertical: 17.8% of the variance) is
 462 accounted for by FCI (50.87%) and D/H (24.58%). All of the models are distinguished on axis

463 1, with a clear separation of the Current model. The five other models form a group
 464 centered on axis 1 and progressively extend toward the right of axis 1. Thus, the Current and
 465 NISPel models show opposite positions on axis 1. The Current model stands out by having
 466 lower TST, AMI, A/C, and $MTL_{3.25}$ than the other models, but a stronger SOI. Thus, in this
 467 model, the lower contribution of trophic level >3.25 seemed to lead energy to flow through
 468 multiple parallel pathways that favored omnivory. On the contrary, in the five other models,
 469 energy was channeled to particular pathways, limiting feeding on several trophic levels (i.e.,
 470 omnivory). The models are not really distinguishable from one other on axis 2, although four
 471 models (ClimOnly, NISMax, NISInt, and NISEqual) seem to present a slightly higher FCI and
 472 D/H ratio.



473
 474 Figure 3: Principal component analysis of the six models (Current, ClimOnly, NISPel, NISEqual,
 475 NISMax, and NISInt) and the eight ENA indices (Total System Throughput, TST; Finn’s Cycling, FCI;
 476 Relative ascendancy, A/C; Averaged Mutual Information, AMI; Mean Trophic Level 2, MTL_2 , Mean
 477 Trophic Level 3.25, $MTL_{3.25}$; System Omnivory Index, SOI; and Detritivory/Herbivory ratio, D/H). Each
 478 model includes all 100 simulations performed with ENATool. The solid dots with a black border
 479 represent the initial models before applying any changes to parameters based on the ENATool
 480 routine. The white dots represent the average model (i.e., the centroid of each model). The table at
 481 the top left shows the absolute contributions of each ENA index for the two axes (in %). The table on
 482 the top left gives information on the percentage contribution of each variable for each dimension.

485 3.2.1. Network ENA

486 TST increased significantly between the Current model and the projected models
 487 (Figure 4, Table 2). The total flux in the system was $6255 (\pm 261) \text{ t.km}^{-2} \cdot \text{year}^{-1}$ in the Current

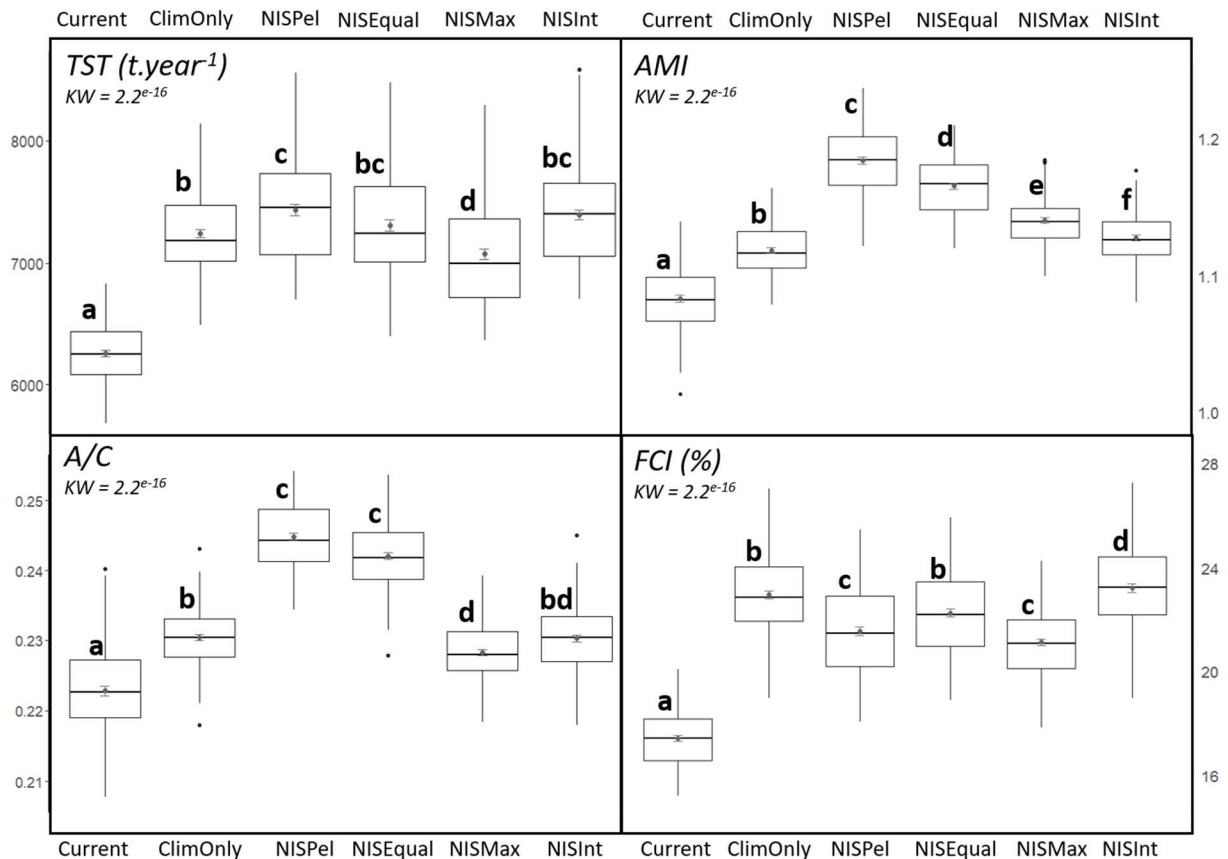
488 model and increased by 15% on average under the future hypotheses. The projected
489 hypotheses presented significantly different TST values, with the exception of NISEqual and
490 NISInt, which showed similar TST.

491 The mean A/C ratio in the Current model was 0.223 and increased significantly up to
492 0.230 under ClimOnly (Figure 4, Table 2). Significant differences were observed between
493 projected models, with the exception of NISPel and NISEqual, which had A/C ratios that were
494 similar and the highest. Mean values of 0.245 and 0.242 were recorded for NISPel and
495 NISEqual, respectively.

496 The AMI increased significantly between the Current model and ClimOnly (Figure 4,
497 Table 2). All NIS hypotheses showed a significantly higher AMI than Current and ClimOnly
498 models. A significant decrease in the AMI value was observed from NISPel (mean of 1.19) to
499 NISInt (mean of 1.13), with intermediate values recorded by NISEqual and NISMax.

500 A significant increase of the FCI was obtained with the projected models (Figure 4,
501 Table 2). The Current model showed a significantly lower FCI value than all the other models
502 (mean of 16.85%). The NISInt model had the highest FCI values followed by ClimOnly and
503 NISEqual, which showed similar FCI. The NISPel and NISMax models had intermediate values
504 between the Current model and the other three models.

505



507
 508 Figure 4: Boxplots of network ENA index values (Total System Throughput, TST; Averaged Mutual
 509 Information, AMI; Relative ascendancy, A/C; and Finn's cycling, FCI), comparing the Current model
 510 and the five projected models (ClimOnly, NISPel, NISEqual, NISMax, and NISInt). The letters
 511 correspond to the significance of the differences between the models, based on a Kruskal–Wallis
 512 (KW) test (p -value < 0.01) and Dunn tests: two models with a different letter are significantly
 513 different. The central dot represents the mean and the standard deviation.
 514

515 According to these results, climate change is expected to cause system productivity
 516 (TST) and recycling (FCI) to increase and to modify the structure of the trophic network (AMI
 517 and A/C). Index values varied greatly according to the NIS model. The highest values of AMI
 518 and A/C for NISPel and NISEqual imply that in these two models, energy would be forced to
 519 flow through direct pathways in order to reach higher trophic levels.
 520

521 3.2.2. Diet ENA

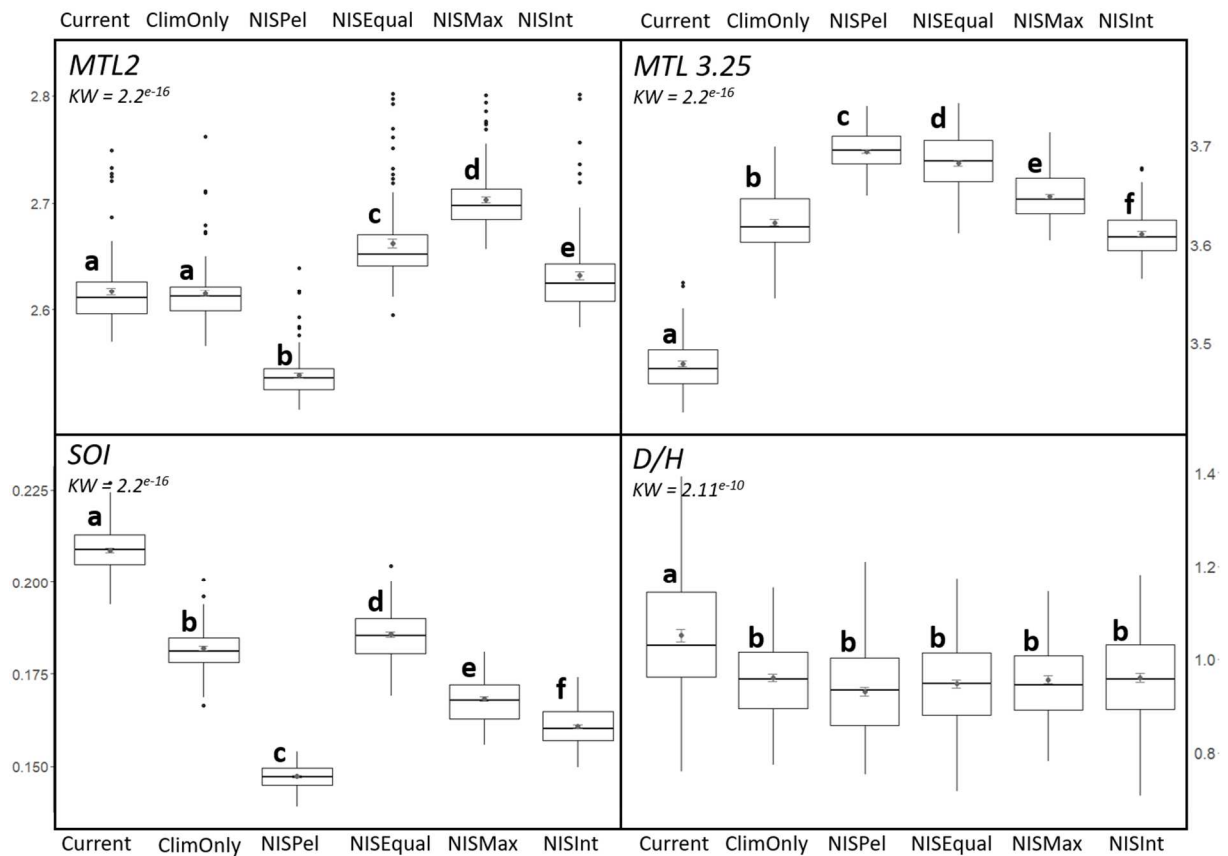
522 There was no significant difference in the MTL_2 of the ClimOnly model compared with
 523 the Current model (Figure 5, Table 2). A significant decrease of MTL_2 was recorded for the
 524 NISPel hypothesis (mean of 2.54) due to the strong increase in biomass of small pelagic fish
 525 of low trophic level such as *Sardinella aurita*. A significant increase was calculated for the
 526 NISEqual and NISMax hypotheses (means of 2.66 and 2.70, respectively), due to the arrival
 527 of non-indigenous demersal benthos feeders and piscivorous fishes, which replaced

528 indigenous species heavily impacted by climate change. The NISInt MTL₂ was slightly higher
529 than the Current and ClimOnly values.

530 The current MTL_{3.25} value (mean 3.48) increased significantly with climate change to
531 reach 3.62 in the ClimOnly model (Figure 5, Table 2). NISPel and NISEqual models showed
532 the highest MTL_{3.25} (means of 3.70 and 3.69, respectively), which can be explained by the
533 increase in fishes of high trophic levels such as tunas for NISPel and demersal piscivorous
534 fishes for NISEqual. The lowest MTL_{3.25} calculated were obtained under the NISInt and
535 NISMax hypotheses (means of 3.61 and 3.65, respectively).

536 The SOI showed a significant decrease between the Current model and all the other
537 projected models (Figure 5, Table 2). There were also significant differences among the
538 future hypotheses. The NISPel model presented the lowest SOI (mean 0.15), whereas the
539 NISEqual model registered the highest among the five future hypothesis values (mean 0.19).
540 However, the NISInt and NISMax values were intermediate (means of 0.16 and 0.17,
541 respectively). The groups with the most marked decrease in omnivory were the top
542 predators (e.g., seabirds, mammals, and sharks) and the pelagic fishes (e.g., planktivores and
543 piscivores) (Table S12 in the Supplementary data).

544 The D/H ratio was significantly lower for the future hypotheses compared with the
545 Current model (Figure 5, Table 2). The decrease in D/H ratio was related to an increase in the
546 flux from primary producers. Detritivory was projected to increase by 4% and herbivory by
547 22% in the future. The increase in herbivory was higher than the increase in detritivory,
548 resulting in a decrease in the D/H ratio.



549
 550 Figure 5: Boxplots of the values of diet ENA indices (Mean Trophic Level 2, MTL₂; Mean Trophic Level
 551 3.25, MTL_{3.25}; System Omnivory Index, SOI; and Detritivory/Herbivory ratio, D/H), comparing the
 552 Current model and the five projected models (ClimOnly, NISPel, NISEqual, NISMax, and NISInt). The
 553 letters correspond to the significance of the differences between the models, based on a Kruskal–
 554 Wallis (KW) test (p-value <0.01) and Dunn tests: models with different letters are significantly
 555 different. The central dot represents the mean and the standard deviation.

556 Climate change is expected to affect the relative contribution of primary producers
 557 and detritus to the feeding of primary consumers. In addition, the effects of both climate
 558 change (i.e., decreased biomass of some groups) and of NIS arrivals would modify trophic
 559 interactions, especially by decreasing the mean omnivory (SOI) in a various ways, according
 560 to the NIS model. The mean trophic level indices (MTL₂ and MTL_{3.25}) showed changes in the
 561 community, with variations according to the trophic functions of arriving NIS.

562 Table 2: Synthesis of trends of ENA indices (Total System Throughput, TST; Finn’s cycling, FCI; Relative
 563 ascendancy, A/C; Averaged Mutual Information, AMI; Mean Trophic Level 2, MTL₂; Mean Trophic
 564 Level 3.25, MTL_{3.25}; System Omnivory Index, SOI; and Detritivory/Herbivory ratio, D/H), comparing
 565 each future model (2041 – 2050) to the Current model (2007 – 2016). The symbol ↗ indicates a
 566 significant increase of the index value in the future model, ↘ represents a significant decrease and
 567 an equal sign '=' means that the Current model and the future model are significantly identical. A
 568 single arrow indicates a slight variation, a double arrow indicates stronger variation and a triple
 569 arrow indicates maximal variation.

570

ENA	ClimOnly	NISPel	NISEqual	NISMax	NISInt
TST	↗↗	↗↗↗	↗↗	↗↗	↗↗
FCI	↗↗	↗↗	↗↗	↗↗	↗↗↗
A/C	↗	↗↗↗	↗↗↗	↗↗	↗↗
AMI	↗	↗↗↗	↗↗	↗↗	↗↗
MTL ₂	=	↘	↗↗	↗↗↗	=
MTL _{3,25}	↗↗	↗↗↗	↗↗	↗↗	↗↗
SOI	↘↘	↘↘↘	↘↘	↘↘	↘↘
D/H	↘	↘	↘	↘	↘

571

572 4. Discussion

573 In this study, we projected the potential response of the Bay of Biscay trophic network to
574 changes in species composition and relative abundances driven by a rise in sea temperature.
575 Our results can be interpreted on three levels. Firstly, [the comparison of ENA indices](#)
576 [between the Current model and the ClimOnly hypothesis gives us information about the](#)
577 [effects of species distribution range reduction due to climate change and increasing](#)
578 [metabolism](#). Secondly, the comparison of ENA indices between the ClimOnly hypothesis and
579 the four others (i.e., NISPel, NISInt, NISEqual, and NISMax) enables us to examine the
580 consequences of NIS arrivals. Finally, the comparison of ENA indices between the Current
581 model and the four NIS hypotheses reveals the combined effects of biomass decreases of
582 some local species and biomass increases of NIS. Several previous studies have investigated
583 the consequences of the arrival of invasive species (Miehls et al., 2009; Baird et al., 2012;
584 Libralato et al., 2015; Goren et al., 2016) or of climate change (Albouy et al., 2014; Raoux et
585 al., 2018; Bourdaud et al., 2021) in food webs structured by native species. A previous study
586 has dealt with the arrival of non-indigenous species in the Mediterranean sea as a result of
587 climate change (Moullec et al., 2019b). These species are expected to arrive due to a
588 northward or southward shift of their range following an increase in water temperature, but
589 are not necessarily expected to become invasive (Lenoir et al., 2020; Urban, 2020).

590

591 4.1. Model limitations

592 We tried to build our models to be as exhaustive as possible. However, some aspects
593 were not taken into account, even though they could play an important role in predicting the
594 future of the ecosystem. Firstly, the models we used did not integrate the organisms'
595 adaption capability. For example, generalist species might experience a diet shift, which
596 would redesign the trophic network. Moreover, the opportunistic processes of fishes and
597 cephalopods in predation cannot be integrated into Ecopath, as the diet matrix is predefined

598 and fixed. Thus, this study does not accurately reflect diet adaptability due to community
599 changes. Furthermore, we did not model a decrease in the native species P/B, even if their
600 biomass declined due to climate change. This suggests that these species are currently at
601 their optimum productivity. Based on this assumption, increasing the native species P/B in
602 the future models as we did hypothesizes that the native species could further develop in
603 the Bay of Biscay and could limit the development of NIS by contrasting with a strong
604 competition. The study of NIS arrivals could be improved by the use of Ecosim and Ecospace.
605 The study could also be improved by forcing the lower trophic level food web according to
606 biogeochemical models. This would make it possible to fit the trophic networks with more
607 realistic phytoplankton and zooplankton biomass variation. Indeed, in the study, we chose to
608 model an increase in primary production, which goes against global projections but follows
609 the trend observed in the Bay of Biscay (Chust et al., 2021). However, as the Bay of Biscay is
610 bottom-up controlled (Corrales et al., 2022), it is vital to obtain reliable results on the
611 evolution of low trophic levels. Also, our models suggest that fishing mortalities would
612 remain constant until the mid-century. However, fisheries management is likely to be
613 adapted to the situation (Badjeck et al., 2010; Quentin Grafton, 2010), especially since the
614 increase in temperature would not impact the stocks in the same way depending on
615 whether the species is stenothermal or eurythermal (Serpetti et al., 2017). Also, our method
616 did not integrate the effects of overfishing of some groups, which can favor NIS to the
617 detriment of native species (Saygu et al., 2020). Furthermore, we assumed that the biomass
618 of native species would decrease proportionally to the reduction of their potential
619 environmental niche, however biomass and environmental niches are not necessarily linked.
620 First, a species will not necessarily use its entire environmental niche: the fact that
621 environmental conditions are favorable in one place does not mean that the species will be
622 present there. Second, biomass does not depend solely on environmental parameters but
623 also on trophic and anthropic factors. Finally, we could not integrate the effects of warming
624 on organism recruitment and spawning, although this has been recorded, for example, on
625 herring in the Celtic Sea (Lauria et al., 2012). Such an effect could indirectly impact biomass
626 and productivity. It is also worth noting that sea temperature affects the organism's length
627 and weight, and the growth coefficient k , which are used in the calculation of P/B (Kielbassa
628 et al., 2010).

629

630 *4.2. The Bay of Biscay trophic network in 2050 under the RCP8.5 scenario*

631 In this section, we compare the Current model with the ClimOnly model. Our results
632 indicate that such ecosystem alterations could increase the quantity of matter flowing
633 through the food web, as suggested by the 15% TST increase by 2050 under RCP8.5 (+0.77°C
634 at the surface). This can, firstly, be explained by the rise in P/B and Q/B. Indeed, despite an
635 observed decrease in total biomass, increasing P/B and Q/B led to higher flux in the system.
636 With the method used in this study, the decline in biomass is due to the decrease in habitat
637 suitability and the increase in P/B and Q/B is due to the rise in sea temperature. This
638 phenomenon is well-known, as marine organisms' metabolic activity is related to

639 temperature (Bruno et al., 2015; Carozza et al., 2019). Warming water is expected to
640 increase P/B and Q/B ratios (Brown et al., 2004). Indeed, respiration and excretion fluxes are
641 projected to rise with sea warming, as already modeled for small pelagic fishes in the Bay of
642 Biscay (Chaalali et al., 2016). Moreover, we forced an increase in the phytoplankton P/B in
643 our model, leading to a higher net primary production in the Bay of Biscay by the mid-
644 century. Thus a higher quantity of matter supported the whole ecosystem. Although several
645 marine biogeochemical models have forecasted a $3.3\% \cdot ^\circ\text{C}^{-1}$ mean global loss of net primary
646 production under RCP8.5, associated with lower diatom biomass (Bopp et al., 2005), these
647 results are often derived from global climate models and do not take into account local
648 specificities (Chust et al., 2014). Some authors have made an assumption of increased
649 primary production. For example, an increase in nutrient concentrations, due to high run-off,
650 would lead to higher primary production (Legge et al., 2020). Moreover, Chust et al. (2021)
651 highlighted an observed increase in primary production in the Bay of Biscay over the last two
652 decades.

653 The intensification of the quantity of matter in the system following temperature increase
654 under RCP8.5 was associated with an increase in recycling index (i.e., FCI), as previously
655 projected by Chaalali et al. (2016), with an increase of 23% in the Bay of Biscay by the end of
656 the century under RCP8.5. A rise in FCI is commonly observed in disturbed ecosystems
657 (Saint-Béat et al., 2015). This increase in FCI values (calculated as the ratio between recycled
658 matter and the TST) despite an increase in TST, means a higher amount of recycled matter.
659 Fath and Halnes (2007) highlighted that flows to and from the detritus compartment are a
660 major part of total structural cycling and an increasing FCI, therefore, results in an increase
661 in detritivory (Fath et al., 2019). Indeed, an increase in detritivory was projected in the Bay
662 of Biscay, although the D/H ratio decreased due to a greater rise in herbivory. The Bay of
663 Biscay could become more dependent on primary production, despite an increase in
664 detritivory. The drop in D/H ratio is also an indicator of stressed ecosystems (Ulanowicz,
665 1997). In our case, the higher rate of herbivory can be explained by the increase in primary
666 production (+2%) and may also be due to the decrease in biomass of some demersal species,
667 which could result in a higher biomass of groups responsible for herbivory fluxes. Increased
668 herbivory may therefore be due to a combination of both the increase in primary production
669 and the decrease in predation. In addition, the increasing FCI can be explained by the
670 increase of bacterial P/B and Q/B associated with a constant biomass in the future models.
671 This supposes that excess bacterial production is consumed, which contributes to the
672 increase of the FCI. Regarding the European landing obligation (i.e., no discards) that was
673 applied in our projected models, this change did not show any influence on the trophic
674 network structure at the scale of the whole Bay of Biscay ecosystem because its contribution
675 to the current flow from detritus was only 0.021%.

676
677 The loss of biomass of some functional groups due to climate change could directly
678 impact the MTL indicators. A constant MTL_2 ($\text{TL} > 2$) associated with an increase in $\text{MTL}_{3.25}$
679 ($\text{TL} > 3.25$) was expected under climate change. This may be explained by the biomass

680 reduction of some trophic groups in intermediate trophic positions, combined with a
681 constant biomass of top predators (TL > 4) such as pelagic fishes (e.g., tunas) and sharks.
682 Indeed, demersal piscivorous fishes (TL = 3.7) were projected to lose 18% of their potential
683 environmental niche by the mid-century under RCP8.5 (Le Marchand et al., 2020). As a
684 result, we reduced their biomass by 18% between the Current model and the future
685 hypotheses. In the same way, flatfish biomass (TL = 3.4) was reduced by 4%. The decrease of
686 these groups' biomass combined with the biomass stability of the top predators (TL > 4),
687 such as pelagic fishes (e.g., tunas) and sharks, led to increased productivity, resulting in a
688 constant MTL₂ associated with an increase in MLT_{3,25} with warming. We should note that this
689 study did not take into account the evolution of fishing pressure, which could alter the
690 community structure. However, the significant increase of the trophic level of demersal
691 fishes observed in the Bay of Biscay, associated with the higher biomass of high trophic level
692 predators (Arroyo et al., 2019), corroborates our results. Moreover, although the
693 opportunistic predation behavior of fishes and cephalopods cannot be integrated into
694 Ecopath, as the diet matrix is predefined and fixed, omnivory (i.e., SOI) was projected to
695 greatly decrease by the mid-century. This result is probably due to the drop in biomass of
696 some prey as well as of predators. For example, the fall in biomass of demersal benthos
697 feeding fishes could reduce their predation by higher trophic level species and could, thus,
698 decrease the omnivory of their predators (i.e., demersal piscivorous fishes). Indeed, the
699 demersal piscivorous omnivory indicator decreased by 44% under the ClimOnly hypothesis
700 (Table S12 in the Supplementary data). Moreover, it is important to note that the omnivory
701 index is calculated based on the trophic level of prey. Thus, all modifications to prey trophic
702 levels may alter the omnivory index value. The decrease in omnivory was associated with a
703 rise in the relative ascendancy. This suggests that parallel pathways (feeding directly or
704 indirectly on a group) tend to disappear. The fall in the biomass of some functional groups
705 could explain this observation. Indeed, energy was weakly channeled to trophic pathways
706 to/from groups whose biomass was altered. As a consequence, other pathways were
707 favored, causing the increase in A/C. The trend in both these ENA indices (i.e., increase in
708 A/C, decrease in SOI) by 2050 under the effect of climate change according to RCP8.5
709 indicates a system becoming simpler by moving towards a chain-like food web.

710

711 *Changes with the arrival of NIS*

712 The arrival of NIS altered energy circulation in the system. It amplified the impact of
713 climate change (ClimOnly) on the AMI. The impact on other network properties depended
714 on the nature of this arrival. ENA indicators are known to be sensitive to environmental
715 specificities and physical parameters, making it difficult to compare ENA values among
716 different ecosystems, but efficient for a "before/after" comparison (Niquil et al.,
717 2012). Indeed, ecosystems are distinguished by specific network properties resulting from
718 interactions between organisms and between these organisms and their environment. These
719 properties affect the ecosystem response to a perturbation, hence the diversity of effect on
720 invasive species. First, the A/C index was very sensitive to the arrival of NIS. The arrivals in

721 the NISPel and NISEqual models could lead to higher A/C and AMI values. This means that
722 these two models could increase the full food-web organization and favor direct pathways to
723 reach higher trophic levels with potentially greater efficiency. Concerning FCI, the variations
724 between the NIS hypotheses highlighted the effects of community composition. Indeed, FCI
725 is strongly correlated with the type of community (Baird et al., 2007). It is worth noting that
726 high biomass of pelagic species (i.e., the NISPel and NISMax hypotheses) induce lower
727 cycling rates. In contrast, higher biomass of demersal species (i.e., the NISEqual model)
728 showed high rates of cycling. Finally, the NISInt model with a low biomass change for both
729 pelagic and demersal species does not seem to affect the cycling rates. It is worth noting
730 that the P/B and Q/B values of NIS were different from those of their mirror groups (Table S5
731 in the Supplementary data), as they were calculated separately for the study. There was no
732 trend in the values. The largest contributors to the flow to detritus under the ClimOnly
733 model were microzooplankton (41%), although this proportion is highly dependent on the
734 structure of the trophic network. The major predator of microzooplankton is
735 mesozooplankton. High consumption of mesozooplankton by planktivorous fishes induces a
736 decrease in predation on microzooplankton. This lessens the flow to detritus by small
737 phytoplankton that are the diet of microzooplankton.

738 The arrival of NIS could amplify the effect of warming on the trophic network
739 structure in the Bay of Biscay due to changes in predation controlled by fish biomass. The
740 MTL of both low trophic level consumers ($TL > 2$) and predators ($TL > 3.25$) could be affected
741 by changes in trophic composition. For example, NISPel is characterized by a drop in MTL_2 (-
742 3% compared with ClimOnly), due to a massive arrival of planktivorous pelagic fishes such as
743 *Sardinella aurita* and *Trachurus traciae* with a low trophic level (respectively 2.5 and 3.3). It
744 should be noted, however, that the amount of zooplankton consumed by *Sardinella aurita*
745 may have been underestimated in our model, giving it a lower trophic level than other
746 planktivorous pelagic fishes such as *Sardina pilchardus* and *Engraulis encrasicolus*. On the
747 contrary, the $MTL_{3.25}$ was very high (+2% compared with ClimOnly), indicating the arrival of
748 top predators such as tunas. The MTL_2 could increase due to a massive arrival of demersal
749 piscivorous species. The significant decrease in the SOI index suggested that the arrival of
750 NIS could amplify the effect of climate change on changes to the trophic network structure.
751 In the Baltic Sea, the arrival of a new predator, an invasive crab (*Rhithropanopeus harrisii*), in
752 a bottom-up controlled ecosystem, has been known to deeply impact both lower trophic
753 levels (by a drop in species richness) and pelagic phytoplankton (by a greater biomass) (Kotta
754 et al., 2018). The NISEqual hypothesis proved that a simple change in marine communities
755 could greatly affect trophic functioning. In the Barents Sea, the observed borealization of
756 Arctic marine communities due to the climate-driven expansion of boreal species is
757 reportedly inducing a deep change in the structure of the current Arctic trophic network
758 (Frainer et al., 2017; Pecuchet et al., 2020; Frainer et al., 2021). In Norway, community
759 changes in the sublittoral area due to kelp expansion induced a change in the trophic
760 structure and its associated flows (Paar et al., 2019). Our results highlighted the issue of NIS,

761 which should be considered more frequently in ecosystem modeling. Indeed, not
762 considering this question may affect ecosystem model projections (Bentley et al., 2017).

763

764 *Combined effects and implications for the trophic network*

765 We expected that a decrease in total biomass and trophic functions due to
766 potentially reduced environmental niches under climate change could be offset by the
767 arrival of NIS. However, our results indicate that whatever the biomass and species arriving
768 in the Bay of Biscay with sea temperature rise, some effects could be observed on the
769 trophic networks. Even in the case of NISEqual, in which the functional groups' losses were
770 replaced in terms of quantity, the trophic network was not projected to return to the current
771 structure. The effects of climate change in the marine realm are often studied individually,
772 whereas these effects are more likely to occur in combination, which could have a more
773 profound impact on ecosystems and fisheries (Ainsworth et al., 2011; Halpern et al., 2015).
774 In terms of the combination of different consequences of climate change, our results
775 support the idea that the ecosystem response is more complex when two or more stressors
776 are associated. The case of the NISEqual hypothesis showed that the arrival of NIS of the
777 same trophic function and in the same proportion could not compensate for the effects of
778 the increase in sea temperature.

779 The cumulative effects of both sea warming and the arrival of NIS could lead to less
780 resistant and less resilient ecosystems in the Bay of Biscay. Even though the interpretation of
781 ENA indicators is often complex (Saint-Béat et al., 2015), our results illustrate major trends.
782 According to Saint-Béat et al. (2015), FCI, SOI, and A/C can be used to estimate the response
783 of a system to a perturbation. In our case, the increase in FCI in the projected models is
784 typical of stressed ecosystems. The disruption of initial recycling has a strong impact on the
785 ecosystem due to the large number of indirect effects associated with cycling (Fath and
786 Halnes, 2007). By indirect effects, the authors referred to paths between two compartments
787 of a length greater than 1. As a consequence, changes in cycling can alter pairwise relations
788 leading to a potential impact on ecosystem response to perturbation such as species
789 invasion, extinction as well as climate change. Omnivory enables the system to adapt to a
790 perturbation by shifts in predator diet. Our results show a large decrease in the omnivory
791 index in the future. The ecosystem could thus be most impacted by the decrease or loss of a
792 species or trophic group, as the ability of a consumer to modulate its diet according to the
793 prey present falls. A decrease in omnivory reduces the flexibility of the system and,
794 therefore, makes it more vulnerable to the disappearance or reduction of biomass of a
795 trophic group. In this way, the consequences for the trophic cascade could have a greater
796 impact (Spiers et al., 2016). However, the combined interpretation of omnivory and A/C
797 shaded this conclusion. The future increase of A/C observed brings the system to a state
798 closer to the "window of vitality" of ecosystems, which defines the optimal range of A/C
799 where the ecosystem is the most sustainable (Fath, 2015). A stress in an ecosystem induces
800 a change in its structure and functioning. In our case, the stress induced by the increase in

801 sea water temperature and the arrival of NIS changes the structure of the trophic network
802 and the way energy enters it. It decreases the capacity of the system to absorb new stresses.
803 The multiplication of pressures on an ecosystem accentuates the consequences of each
804 pressure taken separately (Halpern et al., 2007; Wernberg et al., 2011).

805 **5. Conclusion**

806 This study is timely and important because the cumulative impacts of climate change
807 and non-indigenous species arrivals have rarely been studied in the marine realm. Given
808 uncertainties about non-indigenous species arrivals, simulation through several models was
809 relevant. Indeed, we cannot predict when and which species will enter the area from
810 southern regions under climate change. The models we developed in this study could all
811 represent future realities occurring at different times in the near future. It is possible that
812 NISPel may happen first, then the arrival of demersal with NISEqual and finally the
813 establishment of NIS with high biomass: NISMax. ENA indicators are increasingly used to
814 quantify changes in ecosystems in order to adapt management strategies (Safi et al., 2019).
815 They make it possible to compare a single ecosystem at different levels of change and to
816 compare trends with other ecosystems. The ENATool routine (Guesnet et al., 2015) allowed
817 us to make up for lacking data, especially concerning organism biomass. Our results revealed
818 a negative impact of sea warming on the current trophic network due to the loss of
819 functional group biomass, despite an increase in productivity. The arrival of NIS could imply
820 changes in communities, restructuring the trophic network. Finally, the cumulative effects of
821 both these influences could accentuate trophic network degradation.

822

823 **Acknowledgement**

824 This work was completed as part of the project APPEAL (Socio-ecosystemic approach to the
825 impact of floating wind farms), which benefited from France Energies Marines and State
826 funding managed by the French National Research Agency under the Investments for the
827 Future program, reference ANR- 10-IED-0006-25. M. Le Marchand also benefited from
828 regional funding from *Région Bretagne*.

829

830

831 **References**

832

- 833 Ainsworth, C.H., Samhouri, J.F., Busch, D.S., Cheung, W.W.L., Dunne, J., Okey, T.A., 2011. Potential
834 impacts of climate change on Northeast Pacific marine foodwebs and fisheries. *ICES J. Mar.*
835 *Sci.* 68, 1217–1229. <https://doi.org/10.1093/icesjms/fsr043>
- 836 Albouy, C., Velez, L., Coll, M., Colloca, F., Le Loc'h, F., Mouillot, D., Gravel, D., 2014. From projected
837 species distribution to food-web structure under climate change. *Glob. Change Biol.* 20, 730–
838 741. <https://doi.org/10.1111/gcb.12467>
- 839 Allen, K.R., 1971. Relation Between Production and Biomass. *J. Fish. Res. Board Can.* 28, 1573–1581.
840 <https://doi.org/10.1139/f71-236>
- 841 Arroyo, N.-L., Safi, G., Vouriot, P., López-López, L., Niquil, N., Le Loc'h, F., Hattab, T., Preciado, I.,
842 2019. Towards coherent GES assessments at sub-regional level: signs of fisheries expansion

843 processes in the Bay of Biscay using an OSPAR food web indicator, the mean trophic level.
844 ICES J. Mar. Sci. 76, 1543–1553. <https://doi.org/10.1093/icesjms/fsz023>

845 Badjeck, M.-C., Allison, E.H., Halls, A.S., Dulvy, N.K., 2010. Impacts of climate variability and change
846 on fishery-based livelihoods. *Mar. Policy* 34, 375–383.
847 <https://doi.org/10.1016/j.marpol.2009.08.007>

848 Baird, D., Asmus, H., Asmus, R., 2012. Effect of invasive species on the structure and function of the
849 Sylt-Rømø Bight ecosystem, northern Wadden Sea, over three time periods. *Mar. Ecol. Prog.
850 Ser.* 462, 143–161. <https://doi.org/10.3354/meps09837>

851 Baird, D., Asmus, H., Asmus, R., 2007. Trophic dynamics of eight intertidal communities of the Sylt-
852 Rømø Bight ecosystem, northern Wadden Sea. *Mar. Ecol. Prog. Ser.* 351, 25–41.
853 <https://doi.org/10.3354/meps07137>

854 Baird, D., Asmus, H., Asmus, R., Horn, S., de la Vega, C., 2019. Ecosystem response to increasing
855 ambient water temperatures due to climate warming in the Sylt- Rømø Bight, northern
856 Wadden Sea, Germany. *Estuar. Coast. Shelf Sci.* 228, 106322.
857 <https://doi.org/10.1016/j.ecss.2019.106322>

858 Baird, D., McGlade, J., Ulanowicz, R.E., 1991. The comparative ecology of six marine ecosystems.
859 *Philos. Trans. R. Soc. Lond. B. Biol. Sci.* 333, 15–29. <https://doi.org/10.1098/rstb.1991.0058>

860 Baxter, C.V., Fausch, K.D., Murakami, M., Chapman, P.L., 2004. FISH INVASION RESTRUCTURES
861 STREAM AND FOREST FOOD WEBS BY INTERRUPTING RECIPROCAL PREY SUBSIDIES. *Ecology*
862 85, 2656–2663. <https://doi.org/10.1890/04-138>

863 Bentley, J.W., Serpetti, N., Heymans, J.J., 2017. Investigating the potential impacts of ocean warming
864 on the Norwegian and Barents Seas ecosystem using a time-dynamic food-web model. *Ecol.
865 Model.* 360, 94–107. <https://doi.org/10.1016/j.ecolmodel.2017.07.002>

866 Bopp, L., Aumont, O., Cadule, P., Alvain, S., Gehlen, M., 2005. Response of diatoms distribution to
867 global warming and potential implications: A global model study: DIATOMS AND CLIMATE
868 CHANGE. *Geophys. Res. Lett.* 32, n/a-n/a. <https://doi.org/10.1029/2005GL023653>

869 Bourdaud, P., Ben Rais Lasram, F., Azaïs, E., Champagnat, J., Grusd, S., Halouani, G., Hattab, T.,
870 Leroy, B., Noguès, Q., Raoux, A., Safi, G., Niquil, N., 2021. Impacts of climate change on the
871 Bay of Seine ecosystem: Forcing a spatio-temporal trophic model with predictions from an
872 ecological niche model. *Fish. Oceanogr.* fog.12531. <https://doi.org/10.1111/fog.12531>

873 Brown, J.H., Gillooly, J.F., Allen, A.P., Savage, V.M., West, G.B., 2004. Toward a metabolic theory of
874 ecology. *Ecology* 85, 1771–1789.

875 Bruno, J.F., Carr, L.A., O’Connor, M.I., 2015. Exploring the role of temperature in the ocean through
876 metabolic scaling. *Ecology* 96, 3126–3140. <https://doi.org/10.1890/14-1954.1>

877 Bueno-Pardo, J., García-Seoane, E., Sousa, A.I., Coelho, J.P., Morgado, M., Frankenbach, S., Ezequiel,
878 J., Vaz, N., Quintino, V., Rodrigues, A.M., Leandro, S., Luis, A., Serôdio, J., Cunha, M.R.,
879 Calado, A.J., Lillebø, A., Rebelo, J.E., Queiroga, H., 2018. Trophic web structure and
880 ecosystem attributes of a temperate coastal lagoon (Ria de Aveiro, Portugal). *Ecol. Model.*
881 378, 13–25. <https://doi.org/10.1016/j.ecolmodel.2018.03.009>

882 Butchart, S.H.M., Walpole, M., Collen, B., van Strien, A., Scharlemann, J.P.W., Almond, R.E.A., Baillie,
883 J.E.M., Bomhard, B., Brown, C., Bruno, J., Carpenter, K.E., Carr, G.M., Chanson, J., Chenery,
884 A.M., Csirke, J., Davidson, N.C., Dentener, F., Foster, M., Galli, A., Galloway, J.N., Genovesi, P.,
885 Gregory, R.D., Hockings, M., Kapos, V., Lamarque, J.-F., Leverington, F., Loh, J., McGeoch,
886 M.A., McRae, L., Minasyan, A., Morcillo, M.H., Oldfield, T.E.E., Pauly, D., Quader, S., Revenga,
887 C., Sauer, J.R., Skolnik, B., Spear, D., Stanwell-Smith, D., Stuart, S.N., Symes, A., Tierney, M.,
888 Tyrrell, T.D., Vie, J.-C., Watson, R., 2010. Global Biodiversity: Indicators of Recent Declines.
889 *Science* 328, 1164–1168. <https://doi.org/10.1126/science.1187512>

890 Carozza, D.A., Bianchi, D., Galbraith, E.D., 2019. Metabolic impacts of climate change on marine
891 ecosystems: Implications for fish communities and fisheries. *Glob. Ecol. Biogeogr.* 28, 158–
892 169. <https://doi.org/10.1111/geb.12832>

893 Chaalali, A., Beaugrand, G., Raybaud, V., Lassalle, G., Saint-Béat, B., Le Loc’h, F., Bopp, L., Tecchio, S.,
894 Safi, G., Chifflet, M., Lobry, J., Niquil, N., 2016. From species distributions to ecosystem

895 structure and function: A methodological perspective. *Ecol. Model.* 334, 78–90.
896 <https://doi.org/10.1016/j.ecolmodel.2016.04.022>

897 Cheung, W.W.L., Meeuwig, J.J., Feng, M., Harvey, E., Lam, V.W.Y., Langlois, T., Slawinski, D., Sun, C.,
898 Pauly, D., 2012. Climate-change induced tropicalisation of marine communities in Western
899 Australia. *Mar. Freshw. Res.* 63, 415. <https://doi.org/10.1071/MF11205>

900 Christensen, V., Pauly, D., International Center for Living Aquatic Resources Management,
901 International Council for the Exploration of the Sea, DANIDA (Eds.), 1993. Trophic models of
902 aquatic ecosystems, ICLARM conference proceedings. International Center for Living Aquatic
903 Resources Management ; International Council for the Exploration of the Sea : Danish
904 International Development Agency, Makati, Metro Manila, Philippines : Copenhagen K.,
905 Denmark.

906 Christensen, V., Walters, C.J., 2004. Ecopath with Ecosim: methods, capabilities and limitations. *Ecol.*
907 *Model.* 172, 109–139. <https://doi.org/10.1016/j.ecolmodel.2003.09.003>

908 Christensen, V., Walters, C.J., Pauly, D., 2005. Ecopath with Ecosim: a user's guide. *Fish. Cent. Univ.*
909 *Br. Columbia Vanc.* 154.

910 Chust, G., Allen, J.I., Bopp, L., Schrum, C., Holt, J., Tsiaras, K., Zavatarelli, M., Chifflet, M., Cannaby, H.,
911 Dadou, I., Daewel, U., Wakelin, S.L., Machu, E., Pushpadas, D., Butenschon, M., Artioli, Y.,
912 Petihakis, G., Smith, C., Garçon, V., Goubanova, K., Le Vu, B., Fach, B.A., Salihoglu, B.,
913 Clementi, E., Irigoien, X., 2014. Biomass changes and trophic amplification of plankton in a
914 warmer ocean. *Glob. Change Biol.* 20, 2124–2139. <https://doi.org/10.1111/gcb.12562>

915 Chust, G., González, M., Fontán, A., Revilla, M., Alvarez, P., Santos, M., Cotano, U., Chifflet, M., Borja,
916 A., Muxika, I., Sagarminaga, Y., Caballero, A., de Santiago, I., Epelde, I., Liria, P., Ibaibarriaga,
917 L., Garnier, R., Franco, J., Villarino, E., Irigoien, X., Fernandes-Salvador, J.A., Uriarte, Andrés,
918 Esteban, X., Orue-Echevarria, D., Figueira, T., Uriarte, Adolfo, 2021. Climate regime shifts and
919 biodiversity redistribution in the Bay of Biscay. *Sci. Total Environ.* 149622.
920 <https://doi.org/10.1016/j.scitotenv.2021.149622>

921 Cornou, A-S., Diméet J., Tétard, A., Gaudou, O., Dubé, B., Fauconnet, L., Rochet M-J. 2013.
922 Observations à bord des navires de pêche professionnelle. Bilan de l'échantillonnage 2012. *Obsmer.*

923 Cornou, A-S., Diméet J., Tétard, A., Gaudou, O, Quinio-Scavinner M., Fauconnet L., Dubé B, Rochet M-
924 J. 2015a. Observations à bord des navires de pêche professionnelle. Bilan de l'échantillonnage 2013.
925 *Obsmer.*

926 Cornou A-S, Quinio-Scavinner M, Delaunay D, Diméet J, Goascoz N, Dubé B, Fauconnet L, Rochet M-J
927 2015b. Observations à bord des navires de pêche professionnelle. Bilan de l'échantillonnage 2014.
928 *Obsmer.*

929 Cornou A-S, Diméet J, Goascoz N, Quinio-Scavinner M, Rochet M-J. 2016. Captures et rejets des
930 métiers de pêche français. Résultats des observations à bord des navires de pêche professionnelle en
931 2015. *Obsmer.*

932 Cornou A-S, Goascoz N, Quinio-Scavinner M, Chassanite A, Dubroca L, Rochet M-J. 2017. Captures et
933 rejets des métiers de pêche français. Résultats des observations à bord des navires de pêche
934 professionnelle en 2016. *Obsmer.*

935 Cornou A-S, Goascoz N, Quinio-Scavinner M, Prioul F, Sabbio A, Dubroca L, Renaud F, Rochet M-J.
936 2018. Captures et rejets des métiers de pêche français. Résultats des observations à bord des navires
937 de pêche professionnelle en 2017. *Obsmer.*

938 Corrales, X., Preciado, I., Gascuel, D., Lopez de Gamiz-Zearra, A., Hervann, P.-Y., Mugerza, E.,
939 Louzao, M., Velasco, F., Doray, M., López-López, L., Carrera, P., Cotano, U., Andonegi, E.,
940 2022. Structure and functioning of the Bay of Biscay ecosystem: A trophic modelling
941 approach. *Estuar. Coast. Shelf Sci.* 264, 107658. <https://doi.org/10.1016/j.ecss.2021.107658>

942 Costoya, X., deCastro, M., Gómez-Gesteira, M., Santos, F., 2015. Changes in sea surface temperature
943 seasonality in the Bay of Biscay over the last decades (1982–2014). *J. Mar. Syst.* 150, 91–101.
944 <https://doi.org/10.1016/j.jmarsys.2015.06.002>

945 Delgado, M., Hidalgo, M., Puerta, P., Sánchez-Leal, R., Rueda, L., Sobrino, I., 2018. Concurrent
946 changes in spatial distribution of the demersal community in response to climate variations

947 in the southern Iberian coastal Large Marine Ecosystem. *Mar. Ecol. Prog. Ser.* 607, 19–36.
948 <https://doi.org/10.3354/meps12791>

949 Doney, S.C., Ruckelshaus, M., Emmett Duffy, J., Barry, J.P., Chan, F., English, C.A., Galindo, H.M.,
950 Grebmeier, J.M., Hollowed, A.B., Knowlton, N., Polovina, J., Rabalais, N.N., Sydeman, W.J.,
951 Talley, L.D., 2012. Climate Change Impacts on Marine Ecosystems. *Annu. Rev. Mar. Sci.* 4, 11–
952 37. <https://doi.org/10.1146/annurev-marine-041911-111611>

953 Dubé B, Diméet J, Rochet M-J, Tétard A, Gaudou O, Messannot C, Fauconnet L, Morizur Y, Biseau A,
954 Salaun M. 2012. Observations à bord des navires de pêche professionnelle. Bilan de l'échantillonnage
955 2011. Obsmer

956 Fath, B.D., Asmus, H., Asmus, R., Baird, D., Borrett, S.R., de Jonge, V.N., Ludovisi, A., Niquil, N.,
957 Scharler, U.M., Schückel, U., Wolff, M., 2019. Ecological network analysis metrics: The need
958 for an entire ecosystem approach in management and policy. *Ocean Coast. Manag.* 174, 1–
959 14. <https://doi.org/10.1016/j.ocecoaman.2019.03.007>

960 Fath, B.D., Halnes, G., 2007. Cyclic energy pathways in ecological food webs. *Ecol. Model.* 208, 17–24.
961 <https://doi.org/10.1016/j.ecolmodel.2007.04.020>

962 Fath, B.D., Scharler, U.M., Baird, D., 2013. Dependence of network metrics on model aggregation and
963 throughflow calculations: Demonstration using the Sylt-Rømø Bight Ecosystem. *Ecol. Model.*
964 252, 214–219. <https://doi.org/10.1016/j.ecolmodel.2012.06.010>

965 Fath, B.D., Scharler, U.M., Ulanowicz, R.E., Hannon, B., 2007. Ecological network analysis: network
966 construction. *Ecol. Model.* 208, 49–55. <https://doi.org/10.1016/j.ecolmodel.2007.04.029>

967 Fauconnet L, Badts V, Biseau A, Diméet J, Dintheer C, Dubé B, Gaudou O, Lorange P, Messannot C,
968 Nikolic N, Peronnet I, Reecht Y, Rochet M-J, Tétard A. 2011. Observations à bord des navires de
969 pêche. Bilan de l'échantillonnage 2010. Obsmer.

970 Frainer, A., Primicerio, R., Dolgov, A., Fossheim, M., Johannesen, E., Lind, S., Aschan, M., 2021.
971 Increased functional diversity warns of ecological transition in the Arctic. *Proc. R. Soc. B Biol.*
972 *Sci.* 288, rspb.2021.0054, 20210054. <https://doi.org/10.1098/rspb.2021.0054>

973 Frainer, A., Primicerio, R., Kortsch, S., Aune, M., Dolgov, A.V., Fossheim, M., Aschan, M.M., 2017.
974 Climate-driven changes in functional biogeography of Arctic marine fish communities. *Proc.*
975 *Natl. Acad. Sci.* 114, 12202–12207. <https://doi.org/10.1073/pnas.1706080114>

976 Goren, M., Galil, B.S., Diamant, A., Stern, N., Levitt-Barmats, Y., 2016. Invading up the food web?
977 Invasive fish in the southeastern Mediterranean Sea. *Mar. Biol.* 163, 180.
978 <https://doi.org/10.1007/s00227-016-2950-7>

979 Guesnet, V., Lassalle, G., Chaalali, A., Kearney, K., Saint-Béat, B., Karimi, B., Grami, B., Tecchio, S.,
980 Niquil, N., Lobry, J., 2015. Incorporating food-web parameter uncertainty into Ecopath-
981 derived ecological network indicators. *Ecol. Model.* 313, 29–40.
982 <https://doi.org/10.1016/j.ecolmodel.2015.05.036>

983 Halpern, B.S., Frazier, M., Potapenko, J., Casey, K.S., Koenig, K., Longo, C., Lowndes, J.S., Rockwood,
984 R.C., Selig, E.R., Selkoe, K.A., Walbridge, S., 2015. Spatial and temporal changes in cumulative
985 human impacts on the world's ocean. *Nat. Commun.* 6, 7615.
986 <https://doi.org/10.1038/ncomms8615>

987 Halpern, B.S., Selkoe, K.A., Micheli, F., Kappel, C.V., 2007. Evaluating and Ranking the Vulnerability of
988 Global Marine Ecosystems to Anthropogenic Threats. *Conserv. Biol.* 21, 1301–1315.
989 <https://doi.org/10.1111/j.1523-1739.2007.00752.x>

990 Hirata, H., Ulanowicz, R.E., 1984. Information theoretical analysis of ecological networks. *Int. J. Syst.*
991 *Sci.* 15, 261–270. <https://doi.org/10.1080/00207728408926559>

992 Ifremer 2021. Indices de populations et de communautés issus des campagnes de surveillance
993 halieutique de l'Ifremer. <http://www.ifremer.fr/SIH-indices-campagnes> (08/07/2021)

994 Iglésias, S.P., Lorange, P., 2016. First record of *Pagellus bellottii* (Teleostei: Sparidae) in the Bay of
995 Biscay, France. *Mar. Biodivers. Rec.* 9. <https://doi.org/10.1186/s41200-016-0007-8>

996 Irigoien, X., Chust, G., Fernandes, J.A., Albaina, A., Zarauz, L., 2011. Factors determining the
997 distribution and betadiversity of mesozooplankton species in shelf and coastal waters of the
998 Bay of Biscay. *J. Plankton Res.* 33, 1182–1192. <https://doi.org/10.1093/plankt/fbr026>
999 Kay, J.J., Graham, L.A., Ulanowicz, R.E., 1989. A Detailed Guide to Network Analysis, in: Wulff, F.,
1000 Field, J.G., Mann, K.H. (Eds.), *Network Analysis in Marine Ecology*. Springer Berlin Heidelberg,
1001 Berlin, Heidelberg, pp. 15–61. https://doi.org/10.1007/978-3-642-75017-5_2
1002 Kielbassa, J., Delignette-Muller, M.L., Pont, D., Charles, S., 2010. Application of a temperature-
1003 dependent von Bertalanffy growth model to bullhead (*Cottus gobio*). *Ecol. Model.* 221,
1004 2475–2481. <https://doi.org/10.1016/j.ecolmodel.2010.07.001>
1005 Kotta, J., Wernberg, T., Jänes, H., Kotta, I., Nurkse, K., Pärnoja, M., Orav-Kotta, H., 2018. Novel crab
1006 predator causes marine ecosystem regime shift. *Sci. Rep.* 8, 4956.
1007 <https://doi.org/10.1038/s41598-018-23282-w>
1008 Kwiatkowski, L., Aumont, O., Bopp, L., 2019. Consistent trophic amplification of marine biomass
1009 declines under climate change. *Glob. Change Biol.* 25, 218–229.
1010 <https://doi.org/10.1111/gcb.14468>
1011 Lassalle, G., Lobry, J., Le Loc'h, F., Bustamante, P., Certain, G., Delmas, D., Dupuy, C., Hily, C., Labry,
1012 C., Le Pape, O., Marquis, E., Petitgas, P., Pusineri, C., Ridoux, V., Spitz, J., Niquil, N., 2011.
1013 Lower trophic levels and detrital biomass control the Bay of Biscay continental shelf food
1014 web: Implications for ecosystem management. *Prog. Oceanogr.* 91, 561–575.
1015 <https://doi.org/10.1016/j.pocean.2011.09.002>
1016 Lauria, V., Attrill, M.J., Pinnegar, J.K., Brown, A., Edwards, M., Votier, S.C., 2012. Influence of Climate
1017 Change and Trophic Coupling across Four Trophic Levels in the Celtic Sea. *PLoS ONE* 7,
1018 e47408. <https://doi.org/10.1371/journal.pone.0047408>
1019 Le Marchand, M., Hattab, T., Niquil, N., Albouy, C., Le Loc'h, F., Rais Lasram, F., 2020. Climate change
1020 in the Bay of Biscay: changes in spatial biodiversity patterns could be driven by the arrivals of
1021 southern species. *Mar. Ecol. Prog. Ser.* <https://doi.org/10.3354/meps13401>
1022 Legge, O., Johnson, M., Hicks, N., Jickells, T., Diesing, M., Aldridge, J., Andrews, J., Artioli, Y., Bakker,
1023 D.C.E., Burrows, M.T., Carr, N., Cripps, G., Felgate, S.L., Fernand, L., Greenwood, N., Hartman,
1024 S., Kröger, S., Lessin, G., Mahaffey, C., Mayor, D.J., Parker, R., Queirós, A.M., Shutler, J.D.,
1025 Silva, T., Stahl, H., Tinker, J., Underwood, G.J.C., Van Der Molen, J., Wakelin, S., Weston, K.,
1026 Williamson, P., 2020. Carbon on the Northwest European Shelf: Contemporary Budget and
1027 Future Influences. *Front. Mar. Sci.* 7, 143. <https://doi.org/10.3389/fmars.2020.00143>
1028 Lenoir, J., Bertrand, R., Comte, L., Bourgeaud, L., Hattab, T., Murienne, J., Grenouillet, G., 2020.
1029 Species better track climate warming in the oceans than on land. *Nat. Ecol. Evol.*
1030 <https://doi.org/10.1038/s41559-020-1198-2>
1031 Lercari, D., Defeo, O., Ortega, L., Orlando, L., Gianelli, I., Celentano, E., 2018. Long-term structural and
1032 functional changes driven by climate variability and fishery regimes in a sandy beach
1033 ecosystem. *Ecol. Model.* 368, 41–51. <https://doi.org/10.1016/j.ecolmodel.2017.11.007>
1034 Libralato, S., Caccin, A., Pranovi, F., 2015. Modeling species invasions using thermal and trophic niche
1035 dynamics under climate change. *Front. Mar. Sci.* 2.
1036 <https://doi.org/10.3389/fmars.2015.00029>
1037 Link, J.S., 2010. Adding rigor to ecological network models by evaluating a set of pre-balance
1038 diagnostics: A plea for PREBAL. *Ecol. Model.* 221, 1580–1591.
1039 <https://doi.org/10.1016/j.ecolmodel.2010.03.012>
1040 Lopez y Royo, C., Silvestri, C., Pergent, G., Casazza, G., 2009. Assessing human-induced pressures on
1041 coastal areas with publicly available data. *J. Environ. Manage.* 90, 1494–1501.
1042 <https://doi.org/10.1016/j.jenvman.2008.10.007>
1043 Lotze, H.K., Tittensor, D.P., Bryndum-Buchholz, A., Eddy, T.D., Cheung, W.W., Galbraith, E.D.,
1044 Barange, M., Barrier, N., Bianchi, D., Blanchard, J.L., 2019. Global ensemble projections reveal
1045 trophic amplification of ocean biomass declines with climate change. *Proc. Natl. Acad. Sci.*
1046 116, 12907–12912.

- 1047 Mack, R.N., Simberloff, D., Mark Lonsdale, W., Evans, H., Clout, M., Bazzaz, F.A., 2000. Biotic
1048 invasions: causes, epidemiology, global consequences, and control. *Ecol. Appl.* 10, 689–710.
- 1049 Michel, S., Vandermeersch, F., Lorance, P., 2009. Evolution of upper layer temperature in the Bay of
1050 Biscay during the last 40 years. *Aquat. Living Resour.* 22, 447–461.
1051 <https://doi.org/10.1051/alr/2009054>
- 1052 Miehls, A.L.J., Mason, D.M., Frank, K.A., Krause, A.E., Peacor, S.D., Taylor, W.W., 2009. Invasive
1053 species impacts on ecosystem structure and function: A comparison of Oneida Lake, New
1054 York, USA, before and after zebra mussel invasion. *Ecol. Model.* 220, 3194–3209.
1055 <https://doi.org/10.1016/j.ecolmodel.2009.07.020>
- 1056 Montero-Serra, I., Edwards, M., Genner, M.J., 2015. Warming shelf seas drive the subtropicalization
1057 of European pelagic fish communities. *Glob. Change Biol.* 21, 144–153.
1058 <https://doi.org/10.1111/gcb.12747>
- 1059 Montoya, J.M., Pimm, S.L., Solé, R.V., 2006. Ecological networks and their fragility. *Nature* 442, 259–
1060 264. <https://doi.org/10.1038/nature04927>
- 1061 Moullec, F., Barrier, N., Drira, S., Guilhaumon, F., Marsaleix, P., Somot, S., Ulses, C., Velez, L., Shin, Y.-
1062 J., 2019a. An End-to-End Model Reveals Losers and Winners in a Warming Mediterranean
1063 Sea. *Front. Mar. Sci.* 6, 345. <https://doi.org/10.3389/fmars.2019.00345>
- 1064 Moullec, F., Gascuel, D., Bentorcha, K., Guénette, S., Robert, M., 2017. Trophic models: What do we
1065 learn about Celtic Sea and Bay of Biscay ecosystems? *J. Mar. Syst.* 172, 104–117.
1066 <https://doi.org/10.1016/j.jmarsys.2017.03.008>
- 1067 Moullec, F., Velez, L., Verley, P., Barrier, N., Ulses, C., Carbonara, P., Esteban, A., Follesa, C., Gristina,
1068 M., Jadaud, A., Ligas, A., Díaz, E.L., Maiorano, P., Peristeraki, P., Spedicato, M.T., Thasitis, I.,
1069 Valls, M., Guilhaumon, F., Shin, Y.-J., 2019b. Capturing the big picture of Mediterranean
1070 marine biodiversity with an end-to-end model of climate and fishing impacts. *Prog.*
1071 *Oceanogr.* 178, 102179. <https://doi.org/10.1016/j.pocean.2019.102179>
- 1072 Nehls, G., Diederich, S., Thieltses, D.W., Strasser, M., 2006. Wadden Sea mussel beds invaded by
1073 oysters and slipper limpets: competition or climate control? *Helgol. Mar. Res.* 60, 135–143.
1074 <https://doi.org/10.1007/s10152-006-0032-9>
- 1075 Niquil, N., Arias-González, J.E., Delesalle, B., Ulanowicz, R.E., 1999. Characterization of the planktonic
1076 food web of Takapoto Atoll lagoon, using network analysis. *Oecologia* 118, 232–241.
1077 <https://doi.org/10.1007/s004420050723>
- 1078 Niquil, N., Chaumillon, E., Johnson, G.A., Bertin, X., Grami, B., David, V., Bacher, C., Asmus, H., Baird,
1079 D., Asmus, R., 2012. The effect of physical drivers on ecosystem indices derived from
1080 ecological network analysis: Comparison across estuarine ecosystems. *Estuar. Coast. Shelf*
1081 *Sci.* 108, 132–143. <https://doi.org/10.1016/j.ecss.2011.12.031>
- 1082 Paar, M., de la Vega, C., Horn, S., Asmus, R., Asmus, H., 2019. Kelp belt ecosystem response to a
1083 changing environment in Kongsfjorden (Spitsbergen). *Ocean Coast. Manag.* 167, 60–77.
1084 <https://doi.org/10.1016/j.ocecoaman.2018.09.003>
- 1085 Palomares, M.L.D., Pauly, D., 1998. Predicting food consumption of fish populations as functions of
1086 mortality, food type, morphometrics, temperature and salinity. *Mar. Freshw. Res.* 49, 447.
1087 <https://doi.org/10.1071/MF98015>
- 1088 Parmesan, C., Yohe, G., 2003. A globally coherent fingerprint of climate change impacts across
1089 natural systems. *Nature* 421, 37–42. <https://doi.org/10.1038/nature01286>
- 1090 Pauly, D., 1998. Fishing Down Marine Food Webs. *Science* 279, 860–863.
1091 <https://doi.org/10.1126/science.279.5352.860>
- 1092 Pauly, D., 1980. On the interrelationships between natural mortality, growth parameters, and mean
1093 environmental temperature in 175 fish stocks. *ICES J. Mar. Sci.* 39, 175–192.
1094 <https://doi.org/10.1093/icesjms/39.2.175>
- 1095 Pecuchet, L., Blanchet, M., Fraïner, A., Husson, B., Jørgensen, L.L., Kortsch, S., Primicerio, R., 2020.
1096 Novel feeding interactions amplify the impact of species redistribution on an Arctic food
1097 web. *Glob. Change Biol.* 26, 4894–4906. <https://doi.org/10.1111/gcb.15196>

1098 Poloczanska, E.S., Brown, C.J., Sydeman, W.J., Kiessling, W., Schoeman, D.S., Moore, P.J., Brander, K.,
1099 Bruno, J.F., Buckley, L.B., Burrows, M.T., Duarte, C.M., Halpern, B.S., Holding, J., Kappel, C.V.,
1100 O'Connor, M.I., Pandolfi, J.M., Parmesan, C., Schwing, F., Thompson, S.A., Richardson, A.J.,
1101 2013. Global imprint of climate change on marine life. *Nat. Clim. Change* 3, 919–925.
1102 <https://doi.org/10.1038/nclimate1958>

1103 Quentin Grafton, R., 2010. Adaptation to climate change in marine capture fisheries. *Mar. Policy* 34,
1104 606–615. <https://doi.org/10.1016/j.marpol.2009.11.011>

1105 Raoux, A., Lassalle, G., Pezy, J.-P., Tecchio, S., Safi, G., Ernande, B., Mazé, C., Le Loc'h, F., Lequesne, J.,
1106 Girardin, V., Dauvin, J.-C., Niquil, N., 2018. Measuring sensitivity of two OSPAR indicators for
1107 a coastal food web model under offshore wind farm construction. *Ecol. Indic.*
1108 <https://doi.org/10.1016/j.ecolind.2018.07.014>

1109 Riera, R., Menci, C., Sanabria-Fernández, J.A., Becerro, M.A., 2016. Do recreational activities affect
1110 coastal biodiversity? *Estuar. Coast. Shelf Sci.* 178, 129–136.
1111 <https://doi.org/10.1016/j.ecss.2016.05.022>

1112 Safi, G., Giebels, D., Arroyo, N.L., Heymans, J.J., Preciado, I., Raoux, A., Schückel, U., Tecchio, S., de
1113 Jonge, V.N., Niquil, N., 2019. Vitamine ENA: A framework for the development of ecosystem-
1114 based indicators for decision makers. *Ocean Coast. Manag.* 174, 116–130.
1115 <https://doi.org/10.1016/j.ocecoaman.2019.03.005>

1116 Saint-Béat, B., Baird, D., Asmus, H., Asmus, R., Bacher, C., Pacella, S.R., Johnson, G.A., David, V.,
1117 Vézina, A.F., Niquil, N., 2015. Trophic networks: How do theories link ecosystem structure
1118 and functioning to stability properties? A review. *Ecol. Indic.* 52, 458–471.
1119 <https://doi.org/10.1016/j.ecolind.2014.12.017>

1120 Saygu, İ., Heymans, J.J., Fox, C.J., Özbilgin, H., Eryaşar, A.R., Gökçe, G., 2020. The importance of alien
1121 species to the food web and bottom trawl fisheries of the Northeastern Mediterranean, a
1122 modelling approach. *J. Mar. Syst.* 202, 103253.
1123 <https://doi.org/10.1016/j.jmarsys.2019.103253>

1124 Serpetti, N., Baudron, A.R., Burrows, M.T., Payne, B.L., Helaouët, P., Fernandes, P.G., Heymans, J.J.,
1125 2017. Impact of ocean warming on sustainable fisheries management informs the Ecosystem
1126 Approach to Fisheries. *Sci. Rep.* 7, 13438. <https://doi.org/10.1038/s41598-017-13220-7>

1127 Shannon, L., Coll, M., Bundy, A., Gascuel, D., Heymans, J., Kleisner, K., Lynam, C., Piroddi, C., Tam, J.,
1128 Travers-Trolet, M., Shin, Y., 2014. Trophic level-based indicators to track fishing impacts
1129 across marine ecosystems. *Mar. Ecol. Prog. Ser.* 512, 115–140.
1130 <https://doi.org/10.3354/meps10821>

1131 Taylor, K.E., Stouffer, R.J., Meehl, G.A., 2012. An Overview of CMIP5 and the Experiment Design. *Bull.*
1132 *Am. Meteorol. Soc.* 93, 485–498. <https://doi.org/10.1175/BAMS-D-11-00094.1>

1133 Ulanowicz, R.E., 1986. *Growth and Development*. Springer New York, New York, NY.
1134 <https://doi.org/10.1007/978-1-4612-4916-0>

1135 Urban, M.C., 2020. Climate-tracking species are not invasive. *Nat. Clim. Change* 10, 382–384.
1136 <https://doi.org/10.1038/s41558-020-0770-8>

1137 Vergés, A., Steinberg, P.D., Hay, M.E., Poore, A.G.B., Campbell, A.H., Ballesteros, E., Heck, K.L., Booth,
1138 D.J., Coleman, M.A., Feary, D.A., Figueira, W., Langlois, T., Marzinelli, E.M., Mizerek, T.,
1139 Mumby, P.J., Nakamura, Y., Roughan, M., van Sebille, E., Gupta, A.S., Smale, D.A., Tomas, F.,
1140 Wernberg, T., Wilson, S.K., 2014. The tropicalization of temperate marine ecosystems:
1141 climate-mediated changes in herbivory and community phase shifts. *Proc. R. Soc. B Biol. Sci.*
1142 281, 20140846. <https://doi.org/10.1098/rspb.2014.0846>

1143 Wernberg, T., Russell, B.D., Moore, P.J., Ling, S.D., Smale, D.A., Campbell, A., Coleman, M.A.,
1144 Steinberg, P.D., Kendrick, G.A., Connell, S.D., 2011. Impacts of climate change in a global
1145 hotspot for temperate marine biodiversity and ocean warming. *J. Exp. Mar. Biol. Ecol.* 400, 7–
1146 16. <https://doi.org/10.1016/j.jembe.2011.02.021>

1147

1148